Dynamic transitions and bifurcations for thermal convection in the superposed free flow and porous media

Daozhi Han*, Quan Wang† and Xiaoming Wang‡

February 26, 2020

Abstract

We study the stability and dynamic transitions of thermal convection in a fluid layer overlying a saturated porous media based on the Navier-Stokes-Darcy-Boussinesq model. By reducing the infinite dynamical system to a finite dimensional one via center manifold reduction, we derive a non-dimensional transition number that determines the types of dynamical transitions. We show by careful numerical evaluation of the transition number that the system favours a continuous transition in which the steady state solution bifurcates to a local attractor at the critical Rayleigh number. Jump transitions can occur at certain parameter regime. In particular the jump transition corresponds to the change of flow regime from full convection to free-flow dominated convection at discontinuities of the transition number as a function of the ratio of free-flow to porous media depth, the Darcy number or the thermal diffusivity ratio.

Keywords— Navier-Stokes–Darcy system, thermal convection, porous media, Lions interface boundary conditions, dynamic transition, bifurcation

1 Introduction

The problem of a fluid layer overlying a porous medium has many applications in industrial processes and in geophysical science, including the mixing of surface water and groundwater [4–6], contaminant transport and bioremediation [13, 19], blood flow [20], oil recovery [1, 17, 45] and so on. Of particular interest in this context is the phenomena of thermal convection that has been intensively studied by a number of authors in recent years, cf. [7–9, 14, 23, 24, 26, 31, 42, 43]. In [23] Hill and Straughan compare the linear instability and nonlinear stability thresholds and find excellent agreement between the two based on the Stokes-Darcy-Brinkman model for thermal convection in a fluid overlying a highly porous material. By numerical simulations

*Department of Mathematics and Statistics, Missouri University of Science and Technology, Rolla, MO 65409, USA. Email: *handaoz@mst.edu*

†Department of Mathematics, Sichuan University, Chengdu, China. Email: *xihujunzi@scu.edu.cn*

‡Shanghai Center for Mathematical Sciences and School for Mathematical Sciences, Fudan University, Shanghai 200433 China. Email: *wxm.math@outlook.com*

Carr in [7] studies the onset of convection and the ensuing convection cells in the Navier-Stokes-Darcy model for a layer of fluid superposing a saturated porous medium with internal heating. It is observed that a heat source/sink in the free flow has a destabilizing effect on the porous layer while one in the porous media has a stabilizing effect on the fluid. Very recently Mccurdy et al in [36] perform linear and nonlinear stability analysis on the Navier-Stokes-Darcy model equipped with the nonlinear Lions type interface boundary condition for thermal convection in a coupled free flow-porous media system. In particular they discover through numerical simulation the transition from full convection to free-flow dominated convection at certain parameter regime.

In this article, we aim to study the precise bifurcation and dynamic transitions associated with thermal convection in a fluid layer coupled with a saturated porous medium based on the same Navier-Stokes-Darcy model as the one in [36]. In particular are interested in determining if the transition from one flow regime to another is continuous or jump, in the sense that the state of the flow may gradually or suddenly change from one configuration to another such as the flow regime transition observed in [36]. The approach that we take is the dynamic transition theory developed by Ma and Wang in [35]. According to this theory, dynamic transitions of any dissipative dynamical system can be classified into three categories: continuous, jump, and random. A sufficient condition leading to the existence of a transition in a dissipative system is that the principle of exchange of stabilities (PES) holds true. Roughly speaking, a continuous transition means that the basic state bifurcates to a local attractor; a jump transition says that a system will jump to another state, and a random transition indicates that both continuous and jump transitions are possible depending on the initial perturbation. The theory has been successfully applied in the study of a number of transition problems, including transitions of quasi-geostrophic channel flows [16], instability and transitions of Rayleigh-Benard convection [22, 32, 40, 41], tropical atmospheric circulations [27], dynamic transitions of Cahn-Hilliard equation [29, 30], boundary layer separation [34], and many transition problems with random effects [10–12].

The procedure of the dynamic transition theory is the same as the classical bifurcation theory, and consists of three steps. One first verifies that the PES condition holds true. In general it is difficult to analytically verify the PES condition except in some special cases, see for instance [32, 33]. In the special case of equal thermal diffusivity we rigorously establish the PES condition. In general cases we infer the PES condition by numerically solving the eigenvalue problem. One then reduces the infinite dynamical system to a complex-valued ordinary differential equations via the center manifold reduction. Based on the reduced equation we deduce a transition theorem with a transition number P suitable for numerical computation. Finally one numerically calculates the transition number whose sign determines the type of transition from one state to another. Our numerical evaluation shows that the system prefers a continuous transition in which the steady state solution bifurcates to a local attractor at the critical Rayleigh number. However jump transitions of $P > 0$ nature can indeed occur in certain parameter regime, unlike the transitions associated with classical Rayleigh-Bénard problem in a single domain, cf. [22, 32, 40, 41]. In light of the transition theorem and the numerical evaluation of P we conclude that the jump transition corresponds to the change of flow regime from full convection to free-flow dominated convection at discontinuities of the transition number as a function of

the ratio of free-flow to porous media depth, the Darcy number or the thermal diffusivity ratio.

The article is organized as follows. We provide the mathematical formulation of the problem in Sec. 2. In Sec. 3 we investigate the linear stability, and establish the PES condition analytically and numerically. We perform the center manifold reduction and derive the main transition theorem in Sec. 4. Then we numerically compute the transition number and discuss its physical implications in Sec. 5. Finally we end the article with a summary of the results and open problems in Sec. 6

2 Mathematical formulation

2.1 The model

The physical set-up of the problem is that a layer of fluid overlies a saturated porous medium in which the fluid is heated up at the bottom of the porous medium and cooled off at the top of the free flow region. A schematic description of the problem is shown in Fig. 1. We consider a two dimensional periodic channel with $\Omega_f = \{x \in R, 0 \leq z \leq d_f\}$ for the free flow region and $\Omega_m = \{x \in R, -d_m \leq z \leq 0\}$ for the porous medium region.

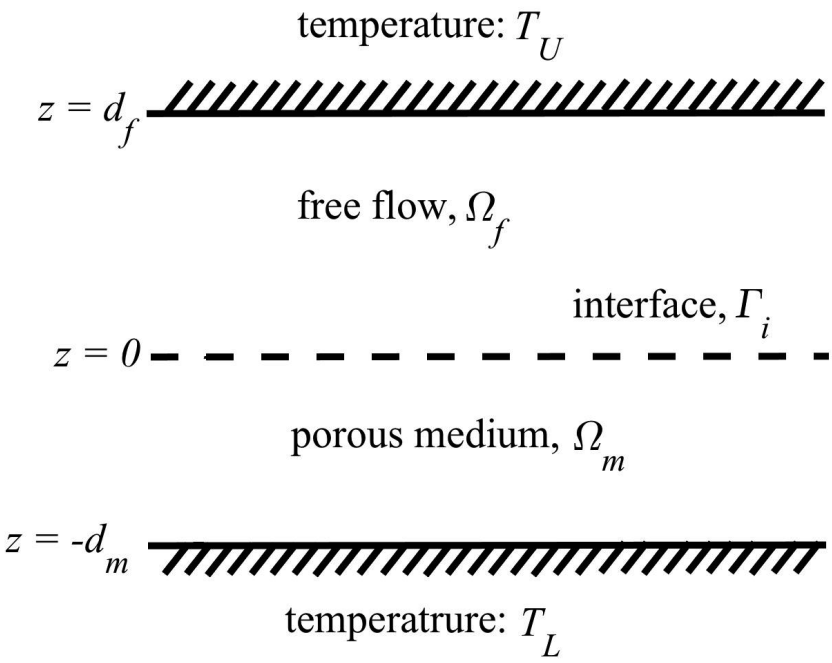

Figure 1: Schematic description of the physical problem. Ω_f: the free flow region; Ω_m: the porous medium; Γ_i: the permeable domain interface. The upper and lower wall are impermeable and maintained at constant temperature with $T_L > T_u$.

The free flow in Ω_f is governed by the Navier-Stokes equation coupled with heat convection–the Boussinesq system:

$$\begin{cases} \rho_0\Big(\frac{\partial \mathbf{u}_f}{\partial t} + (\mathbf{u}_f \cdot \nabla)\mathbf{u}_f\Big) = \nabla \cdot \mathbb{T}(\mathbf{u}_f, p_f) - g\rho_0[1 - \beta(T_f - T_0)]\mathbf{k} \\ \nabla \cdot \mathbf{u}_f = 0, \\ \frac{\partial T_f}{\partial t} + \mathbf{u}_f \cdot \nabla T_f = \frac{\kappa_f}{\rho_0 c_p}\Delta T_f, \\ T_f = T_U, \quad \mathbf{u}_f = 0, \quad \text{at } z = d_f, \end{cases} \tag{2.1}$$

where $\mathbf{u}_f = (u_f, w_f)$, p_f and T_f are the velocity, pressure and temperature of the free flow, respectively; $\mathbb{T}(\mathbf{u}_f, p_f) := 2\mu_0\mathbb{D}(\mathbf{u}_f) - p_f\mathbb{I}$ is the stress tensor with $\mathbb{D}(\mathbf{u}_f) = \frac{1}{2}(\nabla\mathbf{u}_f + \nabla\mathbf{u}_f^T)$ the rate of strain tensor, and μ_0 the dynamic viscosity; ρ_0, β, g and $\mathbf{k}$ are the density, the coefficient of thermal expansion, the gravity constant and the upward unit normal, respectively; κ_f, c_p and $\lambda_f = \frac{\kappa_f}{\rho_0 c_p}$ are the thermal conductivity, specific heat capacity and thermal diffusivity of the fluid, respectively.

The flow in porous media Ω_m is governed by the evolutionary Darcy equation [2, 37]:

$$\begin{cases} \frac{\rho_0}{\chi}\frac{\partial \mathbf{u}_m}{\partial t} + \frac{\mu_0}{\psi}\mathbf{u}_m = -\nabla p_m - g\rho_0[1 - \beta(T_m - T_L)]\mathbf{k}, \\ \nabla \cdot \mathbf{u}_m = 0, \\ \frac{(\rho_0 c_p)_m}{\rho_0 c_p}\frac{\partial T_m}{\partial t} + \mathbf{u}_m \cdot \nabla T_m = \frac{\kappa_m}{\rho_0 c_p}\Delta T_m, \\ T_m = T_L, \quad w_m = 0, \quad \text{at } z = -d_m, \end{cases} \tag{2.2}$$

where $\mathbf{u}_m$, p_m, and T_m are the velocity, pressure and temperature of the fluid in the porous medium; χ and ψ are the porosity and permeability of the porous medium, respectively; $\lambda_m = \frac{\kappa_m}{\rho_0 c_p}$ is the thermal conductivity of fluids in porous media. The heat capacity and thermal conductivity is defined in the sense of harmonic average of that of fluids and solids in the porous medium.

The coupling of the two systems (2.1) and (2.2) is classical, cf. [3, 28, 38]: on the interface $z = 0$,

$$T_f = T_m, \quad \kappa_f\frac{\partial T_f}{\partial z} = \kappa_m\frac{\partial T_m}{\partial z}, \quad w_f = w_m, \tag{2.3a}$$

$$\mu_0\Big(\frac{\partial u_f}{\partial z} + \frac{\partial w_f}{\partial x}\Big) = \frac{\mu_0\alpha}{\sqrt{tr(\psi)}}u_f, \tag{2.3b}$$

$$p_f - 2\mu_0\frac{\partial w_f}{\partial z} + \frac{\rho_0}{2}|\mathbf{u}_f|^2 = p_m. \tag{2.3c}$$

Here the condition (2.3b) are the celebrated Beavers-Joseph-Saffman-Jones (BJSJ) condition with α an empirically determined coefficient and $tr(\psi)$ being the trace of ψ, and the condition (2.3c) is the Lions interface boundary condition.

2.2 The perturbed system

The steady state solution of the system (2.1)–(2.3), denoted with a bar overhead, is given as follows

$$\begin{aligned}
&\overline{\mathbf{u}}_f = \overline{\mathbf{u}}_m = 0,\\
&\overline{T}_f = T_0 + z\frac{T_U - T_0}{d_f},\\
&\overline{T}_m = T_0 + z\frac{T_0 - T_L}{d_m},
\end{aligned} \tag{2.4}$$

with $T_0 = \frac{\kappa_m d_f T_L + \kappa_f d_m T_U}{\kappa_m d_f + \kappa_f d_m}$ being the temperature of the conductive state at $z = 0$. In addition, $\overline{p}_f$ and $\overline{p}_m$ are defined as the hydrostatic pressures such that

$$\begin{aligned}
\nabla \overline{p}_f &= -g\rho_0\big(1 - \beta(\overline{T}_f - T_0)\big)\mathbf{k},\\
\nabla \overline{p}_m &= -g\rho_0\big(1 - \beta(\overline{T}_m - T_L)\big)\mathbf{k}.
\end{aligned}$$

Introducing the perturbations

$$\begin{aligned}
&\mathbf{v}_f = \mathbf{u}_f - \overline{\mathbf{u}}_f, \quad \mathbf{v}_m = \mathbf{u}_m - \overline{\mathbf{u}}_m,\\
&\theta_f = T_f - \overline{T}_f, \quad \theta_m = T_m - \overline{T}_m,\\
&\pi_f = p_f - \overline{p} - f, \quad \pi_m = p_m - \overline{p}_m.
\end{aligned}$$

one finds that the perturbations satisfy the following systems:

$$\begin{cases}
\rho_0\Big(\frac{\partial \mathbf{v}_f}{\partial t} + (\mathbf{v}_f \cdot \nabla)\mathbf{v}_f\Big) = \nabla \cdot \mathbb{T}(\mathbf{v}_f, \pi_f) + g\rho_0\beta\theta_f\mathbf{k}, \quad \text{in } \Omega_f,\\
\nabla \cdot \mathbf{v}_f = 0, \quad \text{in } \Omega_f,\\
\frac{\partial \theta_f}{\partial t} + \mathbf{v}_f \cdot \nabla\theta_f = \lambda_f \Delta\theta_f - w_f\Big(\frac{T_U - T_0}{d_f}\Big), \quad \text{in } \Omega_f,\\
\theta_f = 0, \quad \mathbf{v}_f = 0, \quad \text{at } z = d_f,
\end{cases} \tag{2.5}$$

$$\begin{cases}
\frac{\rho_0}{\chi}\frac{\partial \mathbf{v}_m}{\partial t} + \frac{\mu_0}{\psi}\mathbf{v}_m = -\nabla\pi_m + g\rho_0\beta\theta_m\mathbf{k}, \quad \text{in } \Omega_m,\\
\nabla \cdot \mathbf{u}_m = 0, \quad \text{in } \Omega_m,\\
\frac{(\rho_0 c_p)_m}{\rho_0 c_p}\frac{\partial \theta_m}{\partial t} + \mathbf{v}_m \cdot \nabla\theta_m = \lambda_m \Delta\theta_m - w_m\Big(\frac{T_0 - T_L}{d_m}\Big), \quad \text{in } \Omega_m,\\
T_m = 0, \quad w_m = 0, \quad \text{at } z = -d_m,
\end{cases} \tag{2.6}$$

subject to the interface boundary conditions

$$\begin{cases}
\theta_f = \theta_m, \quad \kappa_f\frac{\partial \theta_f}{\partial z} = \kappa_m\frac{\partial \theta_m}{\partial z}, \quad w_f = w_m, \quad \text{on } z = 0,\\
\mu_0(\frac{\partial u_f}{\partial z} + \frac{\partial w_f}{\partial x}) = \frac{\mu_0\alpha}{\sqrt{tr(\psi)}}u_f, \quad \text{on } z = 0,\\
\pi_f - 2\mu_0\frac{\partial w_f}{\partial z} + \frac{\rho_0}{2}|\mathbf{v}_f|^2 = \pi_m, \quad \text{on } z = 0.
\end{cases} \tag{2.7}$$

2.3 Nondimensionalization

Throughout, denote by $\nu = \frac{\mu_0}{\rho_0}$ the kinematic viscosity. Following [25, 42], we introduce nondimensional variables denoted by tildes

$$\tilde{x}_f = \frac{x_f}{d_f}, \quad \tilde{t} = \frac{t\lambda_f}{d_f^2}, \quad \tilde{\mathbf{v}}_f = \frac{\mathbf{v}_f d_f}{\nu}, \quad \tilde{\theta}_f = \frac{\theta_f \lambda_f}{(T_0 - T_U)\nu}, \quad \tilde{\pi}_f = \frac{\pi_f d_f^2}{\rho_0 \nu^2},$$
$$\tilde{x}_m = \frac{x_m}{d_m}, \quad \tilde{\mathbf{v}}_m = \frac{\mathbf{v}_m d_m}{\nu}, \quad \tilde{\theta}_m = \frac{\theta_m \lambda_m}{(T_L - T_0)\nu}, \quad \tilde{\pi}_m = \frac{\pi_m d_m^2}{\rho_0 \nu^2}.$$

We also introduce the dimensionless numbers

$$\hat{d} = \frac{d_f}{d_m}, \quad \epsilon_T = \frac{\lambda_f}{\lambda_m}, \quad \varrho = \frac{(\rho_0 c_p)_m}{\rho_0 c_p}. \tag{2.8}$$

The periodic cells will still be denoted by $\Omega_f = \{x \in [0, a], z \in [0, 1]\}$ and $\Omega_m = \{x \in [0, b], z \in [-1, 0]\}$ with $b = \hat{d}a$. Then the systems (2.5)–(2.7) take the following dimensionless form (neglecting tildes):

$$\begin{cases} \frac{1}{Pr_f}\frac{\partial \mathbf{v}_f}{\partial t} + (\mathbf{v}_f \cdot \nabla)\mathbf{v}_f = 2\nabla \cdot \mathbb{D}(\mathbf{v}_f) - \nabla \pi_f + Ra_f \theta_f \mathbf{k}, & \text{in } \Omega_f, \\ \nabla \cdot \mathbf{v}_f = 0, & \text{in } \Omega_f, \\ \frac{\partial \theta_f}{\partial t} + Pr_f \mathbf{v}_f \cdot \nabla \theta_f = \Delta \theta_f + w_f, & \text{in } \Omega_f, \\ \theta_f = 0, \quad \mathbf{v}_f = 0, & \text{at } z = 1, \end{cases} \tag{2.9}$$

$$\begin{cases} \frac{\epsilon_T Da}{\hat{d}^2 \chi Pr_m}\frac{\partial \mathbf{v}_m}{\partial t} + \mathbf{v}_m = -Da \nabla \pi_m + Ra_m \theta_m \mathbf{k}, & \text{in } \Omega_m, \\ \nabla \cdot \mathbf{u}_m = 0, & \text{in } \Omega_m, \\ \frac{\epsilon_T \varrho}{\hat{d}^2}\frac{\partial \theta_m}{\partial t} + Pr_m \mathbf{v}_m \cdot \nabla \theta_m = \Delta \theta_m + w_m, & \text{in } \Omega_m, \\ T_m = 0, \quad w_m = 0, & \text{at } z = -1, \end{cases} \tag{2.10}$$

subject to interface boundary conditions

$$\begin{cases} \hat{d}\theta_f = \epsilon_T^2 \theta_m, \quad \frac{\partial \theta_f}{\partial z} = \epsilon_T \frac{\partial \theta_m}{\partial z}, \quad w_f = \hat{d} w_m, & \text{on } z = 0, \\ \frac{\partial u_f}{\partial z} + \frac{\partial w_f}{\partial x} = \frac{\hat{d}\alpha}{\sqrt{Da}} u_f, & \text{on } z = 0, \\ \pi_f - 2\frac{\partial w_f}{\partial z} + \frac{1}{2}|\mathbf{v}_f|^2 = \hat{d}^2 \pi_m, & \text{on } z = 0. \end{cases} \tag{2.11}$$

The dimensionless numbers are defined as follows

$$Pr_f = \frac{\nu}{\lambda_f}, \quad Pr_m = \frac{\nu}{\lambda_m}, \quad Da = \frac{\psi}{d_m^2}, \tag{2.12a}$$
$$Ra_f = \frac{g\beta(T_0 - T_U)d_f^3}{\nu \lambda_f}, \quad Ra_m = \frac{g\beta(T_L - T_0)Dad_m^3}{\nu \lambda_m}, \tag{2.12b}$$

with the relation $Ra_m = \frac{Da\epsilon_T^2}{\hat{d}^4} Ra_f$.

3 Linear stability and principle of exchange of stability

In this article we focus on the transition of the convection dynamics as the control parameter Ra_f (equivalently Ra_m) varies, as well as the influence of other parameters on the dynamic transition. The first step in determining the transition type is to characterize the spectral properties of the linear problem.

The dimensionless linear system associated with the perturbed equations (2.5)–(2.7) take the following form (neglecting tildes):

$$\begin{cases} \frac{1}{Pr_f}\frac{\partial \mathbf{v}_f}{\partial t} = 2\nabla\cdot\mathbb{D}(\mathbf{v}_f) - \nabla\pi_f + Ra_f\theta_f\mathbf{k}, \quad \text{in } \Omega_f, \\ \nabla\cdot\mathbf{v}_f = 0, \quad \text{in } \Omega_f, \\ \frac{\partial\theta_f}{\partial t} = \Delta\theta_f + w_f, \quad \text{in } \Omega_f, \\ \theta_f = 0, \quad \mathbf{v}_f = 0, \quad \text{at } z = 1, \end{cases} \tag{3.13}$$

and

$$\begin{cases} \frac{\epsilon_T Da}{\hat{d}^2\chi Pr_m}\frac{\partial \mathbf{v}_m}{\partial t} + \mathbf{v}_m = -Da\nabla\pi_m + Ra_m\theta_m\mathbf{k}, \quad \text{in } \Omega_m, \\ \nabla\cdot\mathbf{u}_m = 0, \quad \text{in } \Omega_m, \\ \frac{\epsilon\varrho}{\hat{d}^2}\frac{\partial\theta_m}{\partial t} = \Delta\theta_m + w_m, \quad \text{in } \Omega_m, \\ T_m = 0, \quad w_m = 0, \quad \text{at } z = -1, \end{cases} \tag{3.14}$$

subject to the interface boundary conditions

$$\hat{d}\theta_f = \epsilon_T^2\theta_m, \quad \frac{\partial\theta_f}{\partial z} = \epsilon_T\frac{\partial\theta_m}{\partial z}, \quad w_f = \hat{d}w_m, \quad \text{on } z = 0, \tag{3.15}$$

$$\frac{\partial u_f}{\partial z} + \frac{\partial w_f}{\partial x} = \frac{\hat{d}\alpha}{\sqrt{Da}}u_f, \quad \text{on } z = 0,$$

$$\pi_f - 2\frac{\partial w_f}{\partial z} = \hat{d}^2\pi_m, \quad \text{on } z = 0. \tag{3.16}$$

The eigenvalue problem associated with the linear problem (3.13)-(3.16) reads

$$\begin{cases} \frac{\sigma}{Pr_f}\mathbf{v}_f = 2\nabla\cdot\mathbb{D}(\mathbf{v}_f) - \nabla\pi_f + Ra_f\theta_f\mathbf{k}, \quad \text{in } \Omega_f, \\ \sigma\theta_f = \Delta\theta_f + w_f, \quad \text{in } \Omega_f, \\ \nabla\cdot\mathbf{v}_f = 0, \quad \text{in } \Omega_f, \\ \theta_f = 0, \quad \mathbf{v}_f = 0, \quad \text{at } z = 1, \end{cases} \tag{3.17}$$

and

$$\begin{cases} \frac{\sigma\epsilon_T Da}{\hat{d}^2\chi Pr_m}\mathbf{v}_m + \mathbf{v}_m = -Da\nabla\pi_m + Ra_m\theta_m\mathbf{k}, \quad \text{in } \Omega_m, \\ \sigma\frac{\epsilon_T\varrho}{\hat{d}^2}\theta_m = \Delta\theta_m + w_m, \quad \text{in } \Omega_m, \\ \nabla\cdot\mathbf{u}_m = 0, \quad \text{in } \Omega_m, \\ T_m = 0, \quad w_m = 0, \quad \text{at } z = -1, \end{cases} \tag{3.18}$$

which are subject to the same interface boundary conditions (3.15)- (3.16). Following the nondimensionalization in Section 2.3, we note the following relations among the parameters

$$Ra_f = \frac{\hat{d}^4}{Da\epsilon_T^2} Ra_m, \quad Pr_f = \frac{1}{\epsilon_T} Pr_m. \tag{3.19}$$

It is already shown in [36] that there exists a critical Ra_f below which the steady state solution is linearly stable, see also [25]. It is clear that there are countably infinitely many discrete eigenvalues to the problem (3.17)–(3.18), cf. Eqs. (3.34). Let us order the eigenvalues by their decreasing real parts, that is,

$$\operatorname{Re}\sigma_1(Ra_f) \geq \operatorname{Re}\sigma_2(Ra_f) \geq \cdots \to -\infty.$$

We make the standing assumption that the principle of exchange of stability (PES) holds for the eigenvalue problem (3.17)–(3.18). That is, for other parameters fixed there exists a critical Ra_f^0 and a neighborhood Λ_0 of Ra_f^0 such that there exists a unique $m^\star$ with the property that for $Ra_f \in \Lambda_0$

$$\begin{aligned} &\sigma_i(Ra_f) \begin{cases} > 0, & Ra_f > Ra_f^0, \\ = 0, & Ra_f = Ra_f^0, \\ < 0, & Ra_f < Ra_f^0, \end{cases} \qquad 1 \leq i \leq m^\star, \\ &\sigma_j(Ra_f^0) < 0, \quad j \geq m^\star + 1. \end{aligned} \tag{3.20}$$

In general, it is difficult to verify analytically the PES condition, due to the lack of explicit form of the eigenvalues and eigenfunctions. We shall demonstrate the validity of the PES condition by numerically solving the eigenvalue problem at the end of this section. Nonetheless, for the special case $\epsilon_T = 1$, i.e. identical thermal conductivity between the free flow and porous media, we can rigorously establish the PES condition.

3.1 PES condition when $\epsilon_T = 1$

Let us define some function spaces as follows

$$\begin{aligned} &\mathbf{X}_f = \left\{ \mathbf{v} \in \mathbf{H}^1(\Omega_f) \,\middle|\, \nabla \cdot \mathbf{v} = 0, \quad \mathbf{v}|_{z=1} = 0, \quad \text{periodic in } x \right\}, \\ &\mathbf{X}_m = \left\{ \mathbf{v} \in \mathbf{H}^1(\Omega_m) \,\middle|\, \nabla \cdot \mathbf{v} = 0, \quad \mathbf{v} \cdot \mathbf{n}|_{z=-1} = 0, \quad \text{periodic in } x \right\}, \\ &Y_f = \left\{ \theta \in H^1(\Omega_f) \,\middle|\, \theta|_{z=1} = 0, \quad \text{periodic in } x \right\}, \\ &Y_m = \left\{ \theta \in H^1(\Omega_m) \,\middle|\, \theta|_{z=-1} = 0, \quad \text{periodic in } x \right\}, \\ &\overline{\mathbf{X}}_f = \left\{ \mathbf{v} \in \mathbf{L}^2(\Omega_f) \,\middle|\, \text{periodic in } x \right\}, \quad \overline{\mathbf{X}}_m = \left\{ \mathbf{v} \in \mathbf{L}^2(\Omega_m) \,\middle|\, \text{periodic in } x \right\}, \\ &\overline{Y}_f = \left\{ \theta \in L^2(\Omega_f) \,\middle|\, \text{periodic in } x \right\}, \quad \overline{Y}_m = \left\{ \theta \in L^2(\Omega_m) \,\middle|\, \text{periodic in } x \right\}, \end{aligned} \tag{3.21}$$

$$\mathbf{X} = \left\{ \mathbf{U} = (\mathbf{v}_f, \theta_f, \mathbf{v}_m, \theta_m) \in \mathbf{X}_f \times Y_f \times \mathbf{X}_m \times Y_m \middle| \mathbf{U} \text{ satisfying (3.15)} \right\}, \tag{3.22}$$

$$\mathbf{Y} = \left\{ (\mathbf{v}_f, \theta_f, \mathbf{v}_m, \theta_m) \in \overline{\mathbf{X}}_f \times \overline{Y}_f \times \overline{\mathbf{X}}_m \times \overline{Y}_m \right\}. \tag{3.23}$$

In case of $\epsilon_T = 1$, the following theorem holds.

Theorem 3.1. *If $\epsilon_T = 1$, then all eigenvalues of the eigenvalue problem (3.17)-(3.18) are real, and the principle of exchange of stability (3.20) holds.*

Proof. First we show that the eigenvalues are real. It follows from the equations (3.17)-(3.18) that

$$\begin{aligned}
&\hat{d}\left(\frac{\sigma}{Pr_f}\mathbf{v}_f, \overline{\mathbf{v}}_f\right) + Ra_f\hat{d}\sigma\left(\theta_f, \overline{\theta}_f\right) \\
&+ \frac{\sigma\hat{d}^2\epsilon_T}{\chi Pr_m}\left(\mathbf{v}_m, \overline{\mathbf{v}}_m\right) + \sigma Ra_f\frac{\epsilon_T^4\varrho}{\hat{d}^2}\left(\theta_m, \overline{\theta}_m\right) \\
&= 2\hat{d}\left(\nabla\cdot\mathbb{D}(\mathbf{v}_f) - \nabla\pi_f + Ra_f\theta_f\mathbf{k}, \overline{\mathbf{v}}_f\right) + Ra_f\hat{d}\left(\Delta\theta_f + w_f, \overline{\theta}_f\right) \\
&+ \frac{\hat{d}^4}{Da}\left(-Da\nabla\pi_m - \mathbf{v}_m + Ra_m\theta_m\mathbf{k}, \overline{\mathbf{v}}_m\right) + Ra_f\epsilon_T^3\left(\Delta\theta_m + w_m, \overline{\theta}_m\right),
\end{aligned} \tag{3.24}$$

where the variables with overlines are their complex conjugate.

Utilizing the interface boundary conditions (3.15)- (3.16), one calculates

$$\begin{aligned}
&2\hat{d}\left(\nabla\cdot\mathbb{D}(\mathbf{v}_f) - \nabla\pi_f + Ra_f\theta_f\mathbf{k}, \overline{\mathbf{v}}_f\right) + Ra_f\hat{d}\left(\Delta\theta_f + w_f, \overline{\theta}_f\right) \\
&+ \frac{\hat{d}^4}{Da}\left(-Da\nabla\pi_m - \mathbf{v}_m + Ra_m\theta_m\mathbf{k}, \overline{\mathbf{v}}_m\right) + Ra_f\epsilon_T^3\left(\Delta\theta_m + w_m, \overline{\theta}_m\right) \\
&= -2\hat{d}(\mathbb{D}(\mathbf{v}_f), \mathbb{D}(\overline{\mathbf{v}}_f)) + \hat{d}(Ra_f\theta_f, \overline{w}_f) - \frac{\hat{d}^4}{Da}(\mathbf{v}_m, \overline{\mathbf{v}}_m) + \frac{\hat{d}^4 Ra_m}{Da}(\theta_m, \overline{w}_m) \\
&\quad - Ra_f\hat{d}(\nabla\theta_f, \nabla\overline{\theta}_f) + \hat{d}Ra_f(\overline{\theta}_f, w_f) - Ra_f\epsilon_T^3(\nabla\theta_m, \nabla\overline{\theta}_m) + Ra_f\epsilon_T^3(\overline{\theta}_m, w_m) \\
&\quad - 2\frac{\hat{d}^2\alpha}{\sqrt{Da}}\sum_{s=1}^{2}\int_{\Gamma_i}(\mathbf{v}_f\cdot\tau_s)(\overline{\mathbf{v}}_f\cdot\tau_s)\,d\Gamma_i - \hat{d}\int_{\Gamma_i}\left(2\frac{\partial w_f}{\partial z} - \pi_f + \hat{d}^2\pi_m\right)(\overline{\mathbf{v}}_f\cdot\mathbf{n})\,d\Gamma_i \\
&\quad - Ra_f\hat{d}\int_{\Gamma_i}\theta_f(\nabla\overline{\theta}_f\cdot\mathbf{n})\,d\Gamma_i + Ra_f\epsilon_T^3\int_{\Gamma_i}\theta_m(\nabla\overline{\theta}_m\cdot\mathbf{n})\,d\Gamma_i \\
&= -2\hat{d}(\mathbb{D}(\mathbf{v}_f), \mathbb{D}(\overline{\mathbf{v}}_f)) - Ra_f\hat{d}(\nabla\theta_f, \nabla\overline{\theta}_f) - \frac{\hat{d}^4}{Da}(\mathbf{v}_m, \overline{\mathbf{v}}_m) - Ra_f\epsilon_T^3(\nabla\theta_m, \nabla\overline{\theta}_m) \\
&\quad + \frac{\hat{d}^4 Ra_m}{Da}(\theta_m, \overline{w}_m) + \hat{d}Ra_f(\theta_f, \overline{w}_f) + \hat{d}Ra_f(\overline{\theta}_f, w_f) + Ra_f\epsilon_T^3(\overline{\theta}_m, w_m) \\
&\quad - 2\frac{\hat{d}^2\alpha}{\sqrt{Da}}\sum_{s=1}^{2}\int_{\Gamma_i}(\mathbf{v}_f\cdot\tau_s)(\overline{\mathbf{v}}_f\cdot\tau_s)\,d\Gamma_i \\
&= -2\hat{d}(\mathbb{D}(\mathbf{v}_f), \mathbb{D}(\overline{\mathbf{v}}_f)) - Ra_f\hat{d}(\nabla\theta_f, \nabla\overline{\theta}_f) - \frac{\hat{d}^4}{Da}(\mathbf{v}_m, \overline{\mathbf{v}}_m) - Ra_f\epsilon_T^3(\nabla\theta_m, \nabla\overline{\theta}_m) \\
&\quad + \hat{d}Ra_f(\theta_f, \overline{w}_f) + \hat{d}Ra_f(w_f, \overline{\theta}_f) + Ra_f\epsilon_T^2(\theta_m, \overline{w}_m) + Ra_f\epsilon_T^3(w_m, \overline{\theta}_m) \\
&\quad - 2\frac{\hat{d}^2\alpha}{\sqrt{Da}}\sum_{s=1}^{2}\int_{\Gamma_i}(\mathbf{v}_f\cdot\tau_s)(\overline{\mathbf{v}}_f\cdot\tau_s)\,d\Gamma_i,
\end{aligned} \tag{3.25}$$

where the relation $Ra_m = \frac{Da\epsilon_T^2}{\hat{d}^4}Ra_f$ has been applied in the derivation of last equation. Thus, if $\epsilon_T = 1$, then Eqs. (3.24) and (3.25) imply that the eigenvalues σ are real.

We now establish the PES condition (3.20) under the assumption $\epsilon_T = 1$. By direct energy estimates (cf. [36]), one can show that the system (2.9)-(2.10) subject to the interface boundary conditions (3.15)-(3.16) is energy stable for $Ra_f < R_0$. Hence the steady-state (2.4) is linearly stable if the Rayleigh number $Ra_f < R_0$. For the study of bifurcation/transition, one assumes that $Ra_f \geq R_0 > 0$.

First let us re-scale θ_f and θ_m by $\sqrt{Ra_f}$. Then (3.17)-(3.18) becomes

$$\begin{cases} \frac{\sigma}{Pr_f}\mathbf{v}_f = 2\nabla\cdot\mathbb{D}(\mathbf{v}_f) - \nabla\pi_f + \sqrt{Ra_f}\theta_f\mathbf{k}, \quad \text{in } \Omega_f, \\ \sigma\theta_f = \Delta\theta_f + \sqrt{Ra_f}w_f, \quad \text{in } \Omega_f, \\ \nabla\cdot\mathbf{v}_f = 0, \quad \text{in } \Omega_f, \\ \theta_f = 0, \quad \mathbf{v}_f = 0, \quad \text{at } z = 1, \end{cases} \tag{3.26}$$

and

$$\begin{cases} \frac{\sigma\epsilon_T Da}{\hat{d}^2\chi Pr_m}\mathbf{v}_m + \mathbf{v}_m = -Da\nabla\pi_m + \frac{Ra_m}{\sqrt{Ra_f}}\theta_m\mathbf{k}, \quad \text{in } \Omega_m, \\ \sigma\frac{\epsilon_T\varrho}{\hat{d}^2}\theta_m = \Delta\theta_m + \sqrt{Ra_f}w_m, \quad \text{in } \Omega_m, \\ \nabla\cdot\mathbf{u}_m = 0, \quad \text{in } \Omega_m, \\ T_m = 0, \quad w_m = 0, \quad \text{at } z = -1, \end{cases} \tag{3.27}$$

subject to the same interface conditions. We proceed to show that the principle of exchange of stability (3.20) holds for the eigenvalue problem (3.26)-(3.27) in two steps.

Step 1: Existence of a critical Ra_f^0. Under the assumption that $\epsilon_T = 1$, the weak form of the eigenvalue problem (3.26)-(3.27) can be written as

$$\begin{aligned} &\frac{\hat{d}\sigma}{Pr_f}\left(\mathbf{v}_f, \mathbf{v}_f'\right) + \hat{d}\sigma\left(\theta_f, \theta_f'\right) + \frac{\sigma\epsilon_T\hat{d}^2}{\chi Pr_m}\left(\mathbf{v}_m, \mathbf{v}_m'\right) + \sigma\frac{\epsilon_T\varrho}{\hat{d}^2}\left(\theta_m, \theta_m'\right) \\ &= -2\hat{d}\big(\mathbb{D}(\mathbf{v}_f), \mathbb{D}(\mathbf{v}_f')\big), -\hat{d}(\nabla\theta_f, \nabla\theta_f') - \frac{\hat{d}^4}{Da}(\mathbf{v}_m, \mathbf{v}_m') - (\nabla\theta_m, \nabla\theta_m') \\ &\quad + \hat{d}\sqrt{Ra_f}(\theta_f, w_f') + \hat{d}\sqrt{Ra_f}(w_f, \theta_f') + \sqrt{Ra_f}(\theta_m, w_m') + \sqrt{Ra_f}(w_m, \theta_m') \\ &\quad - 2\frac{\hat{d}^2\alpha}{\sqrt{Da}}\sum_{s=1}^{2}\int_{\Gamma_i}(\mathbf{v}_f\cdot\tau_s)(\mathbf{v}_f'\cdot\tau_s)\,d\Gamma_i, \quad \forall\mathbf{U}'\in\mathbf{X}. \end{aligned} \tag{3.28}$$

We show that there exists a critical $Ra_f = Ra_f^0 > 0$ such that the eigenvalue problem (3.28) has zero eigenvalues, i.e. $\sigma = 0$.

For convenience, let $L_{Ra_f} = A + \sqrt{Ra_f}B$ be the operator from $\mathbf{X}$ to its dual space $\mathbf{X}^*$, with A and B induced respectively by the right-hand side of Eq. (3.28)

$$\begin{aligned} \langle A\mathbf{U}, \mathbf{U}'\rangle =& -2\hat{d}\Big(\mathbb{D}(\mathbf{v}_f), \mathbb{D}(\mathbf{v}_f')\Big) - \hat{d}(\nabla\theta_f, \nabla\theta_f') - \frac{\hat{d}^4}{Da}(\mathbf{v}_m, \mathbf{v}_m') - (\nabla\theta_m, \nabla\theta_m') \\ &- 2\frac{\hat{d}^2\alpha}{\sqrt{Da}}\sum_{s=1}^{2}\int_{\Gamma_i}(\mathbf{v}_f\cdot\tau_s)(\mathbf{v}_f'\cdot\tau_s)\,d\Gamma_i, \\ \langle B\mathbf{U}, \mathbf{U}'\rangle =& \hat{d}(\theta_f, w_f') + \hat{d}(w_f, \theta_f') + (\theta_m, w_m') + (w_m, \theta_m'). \end{aligned}$$

In light of the relation (3.19), the weak form of the eigenvalue problem (3.28) is equivalent to

$$L_{Ra_f}\mathbf{U} = \sigma M\mathbf{U}, \quad \text{in } \mathbf{X}, \tag{3.29}$$

with

$$\mathbf{M}=\begin{pmatrix} \frac{\hat{d}}{Pr_f} & 0 & 0 & 0 & 0 & 0 \\ 0 & \frac{\hat{d}}{Pr_f} & 0 & 0 & 0 & 0 \\ 0 & 0 & \hat{d} & 0 & 0 & 0 \\ 0 & 0 & 0 & \frac{\hat{d}^2}{\chi Pr_m} & 0 & 0 \\ 0 & 0 & 0 & 0 & \frac{\hat{d}^2}{\chi Pr_m} & 0 \\ 0 & 0 & 0 & 0 & 0 & \frac{\varrho}{\hat{d}^2} \end{pmatrix}.$$

By the symmetry of the operator L_{Ra_f}, the first eigenvalue $\sigma_{f,1}$ is characterized by

$$\begin{aligned} \sigma_{f,1} &= \max_{\|U\|_{\mathbf{X}}=1} \langle M^{-1}(L_{Ra_f}\mathbf{U}),\mathbf{U}\rangle \\ &= \max_{\|U\|_{\mathbf{X}}=1} \Big(\langle M^{-1}(A\mathbf{U}),\mathbf{U}\rangle + \sqrt{Ra_f}\langle (M^{-1}(B\mathbf{U}),\mathbf{U})\rangle\Big). \end{aligned} \tag{3.30}$$

Note that

$$\langle A\mathbf{U},\mathbf{U}\rangle < 0, \quad \forall \mathbf{U}\in\mathbf{X}. \tag{3.31}$$

Also

$$\langle B\mathbf{U},\mathbf{U}\rangle > 0, \tag{3.32}$$

for $\mathbf{U}=(\mathbf{v}_f,\theta_f,\mathbf{v}_m,\theta_m)$ such that

$$w_f=\theta_f, \quad w_m=\theta_m, \quad \text{with} \quad w_f\neq 0 \quad \text{or} \quad w_m\neq 0.$$

Hence, one can deduce from (3.30)-(3.32) that there exists $Ra_f = Ra_f^0 > 0$ such that the first eigenvalue associated with the eigenvalue problem (3.29) vanishes, i.e.,

$$\sigma_1 = 0.$$

Step 2: The transversal condition. We show that the first eigenvalue $\sigma_i(Ra_f), i=1,\cdots m$ counting multiplicity satisfies

$$(\sigma_i(Ra_f))'\big|_{Ra_f=Ra_f^0} > 0. \tag{3.33}$$

To this end, let

$$L_{Ra_f^0+\delta}\mathbf{U_1} = \sigma_i(Ra_f^0+\delta)M\mathbf{U_1}, \quad \mathbf{U_1}=\mathbf{U}_{Ra_f^0}+\mathbf{U}_\delta, \quad \lim_{\delta\to 0}\mathbf{U}_\delta=\mathbf{0},$$

where $L_{Ra_f^0}\mathbf{U}_{Ra_f^0}=\mathbf{0}$. One calculates

$$\begin{aligned} \left\langle L_{Ra_f^0+\delta}\mathbf{U_1},\mathbf{U}_{Ra_f^0}\right\rangle &= \left\langle L_{Ra_f^0}\mathbf{U}_{Ra_f^0},\mathbf{U}_{Ra_f^0}\right\rangle + \left\langle L_{Ra_f^0}\mathbf{U}_\delta,\mathbf{U}_{Ra_f^0}\right\rangle \\ &\quad + \left\langle \left(L_{Ra_f^0+\delta}-L_{Ra_f^0}\right)\mathbf{U}_1,\mathbf{U}_{Ra_f^0}\right\rangle \\ &= \left(\sqrt{Ra_f^0+\delta}-\sqrt{Ra_f^0}\right)\left\langle B\mathbf{U}_1,\mathbf{U}_{Ra_f^0}\right\rangle, \end{aligned}$$

where the identity

$$\left\langle L_{Ra_f^0}\mathbf{U}_\delta, \mathbf{U}\right\rangle = \left\langle \mathbf{U}_\delta, L_{Ra_f^0}\mathbf{U}\right\rangle = 0,$$

has been used. On the other hand,

$$\left\langle L_{Ra_f^0+\delta}\mathbf{U_1}, \mathbf{U}_{Ra_f^0}\right\rangle = \sigma_i(Ra_f^0+\delta)\left\langle M\mathbf{U_1}, \mathbf{U}_{Ra_f^0}\right\rangle.$$

Hence

$$\left(\sqrt{Ra_f^0+\delta}-\sqrt{Ra_f^0}\right)\left\langle B\mathbf{U}_1, \mathbf{U}_{Ra_f^0}\right\rangle = \sigma_i(Ra_f^0+\delta)\left\langle M\mathbf{U_1}, \mathbf{U}_{Ra_f^0}\right\rangle.$$

And therefore

$$\begin{aligned}\frac{\left(\sqrt{Ra_f^0+\delta}-\sqrt{Ra_f^0}\right)}{\delta}\left\langle B\mathbf{U}_1, \mathbf{U}_{Ra_f^0}\right\rangle &= \frac{\sigma_i(Ra_f^0+\delta)}{\delta}\left\langle M\mathbf{U_1}, \mathbf{U}_{Ra_f^0}\right\rangle \\ &= \frac{\sigma_i(Ra_f^0+\delta)-\sigma_i(Ra_f^0)}{\delta}\left\langle M\mathbf{U_1}, \mathbf{U}_{Ra_f^0}\right\rangle,\end{aligned}$$

which yields

$$(\sigma_i(Ra_f))'\big|_{Ra_f=Ra_f^0} = \frac{\left\langle B\mathbf{U}_{Ra_f^0}, \mathbf{U}_{Ra_f^0}\right\rangle}{2\sqrt{Ra_f^0}\left\langle M\mathbf{U}_{Ra_f^0}, \mathbf{U}_{Ra_f^0}\right\rangle} > 0.$$

This establishes (3.33).

The proof of (3.20) is now complete. □

3.2 Numerical solution of the eigenvalue problem

In this subsection we numerically solve the eigenvalue problem (3.17)–(3.18). The numerical results would allow us to demonstrate the validity of the PES condition. Furthermore, the eigenfunctions are needed in the numerical evaluation of the transition number.

Owing to the periodic boundary conditions in the horizontal direction and the separable form of the equations, the following normal mode solutions can be assumed for fluid in Ω_f

$$\begin{aligned}&\mathbf{v}_f = \mathbf{v}_f(z)\exp\left(\sigma t + i2n\pi/ax\right), \quad \pi_f = \pi_f(z)\exp\left(\sigma t + i2n\pi/ax\right)\\ &\theta_f = \theta_f(z)\exp\left(\sigma t + i2n\pi/ax\right), \quad n\in\mathbb{Z}.\end{aligned}$$

The normal mode solutions for fluid in Ω_m is similarly defined. One then eliminates the pressure term by taking curl of the fluid equation, and derives the equation for the component $w_i, i \in \{f, m\}$ after taking another curl of the resulting equation, cf. ([18] p. 96) for details. The interface boundary conditions are written in terms of $w_i, i \in \{f, m\}$ as well with the aid of the fluid equations.

Introducing the notations

$$D := \frac{d}{dz}, \quad a_n^2 = \left(2n\pi/a\right)^2, \quad b_n^2 = \left(2n\pi/b\right)^2,$$

the eigenvalue problem becomes (see also [23]):

$$\begin{cases}\sigma_n\mathcal{A}_n^f\psi_f = \mathcal{L}_n^f\psi_f, \quad \psi_f = (w_f, \theta_f), \quad z\in(0,1),\\ \sigma_n\mathcal{A}_n^m\psi_m = \mathcal{L}_n^m\psi_m, \quad \psi_m = (w_m, \theta_m), \quad z\in(-1,0),\\ w_f = Dw_f = \theta_f = 0, \quad z = 1,\\ w_m = \theta_m = 0, \quad z = -1,\end{cases} \tag{3.34}$$

where

$$\mathcal{A}_n^f\psi_f = \begin{pmatrix} \frac{1}{Pr_f}(D^2-a_n^2)w_f \\ \theta_f \end{pmatrix}, \quad \mathcal{L}_n^f\psi_f = \begin{pmatrix} (D^2-a_n^2)^2 w_f - a_n^2 Ra_f\theta_f \\ (D^2-a_n^2)\theta_f + w_f \end{pmatrix}, \tag{3.35}$$

$$\mathcal{A}_n^m\psi_m = \begin{pmatrix} \frac{\epsilon_T Da}{\hat{d}^2\chi Pr_m}(D^2-b_n^2)w_m \\ \frac{\epsilon_T\varrho}{\hat{d}^2}\theta_m \end{pmatrix}, \quad \mathcal{L}_n^m\psi_m = \begin{pmatrix} -(D^2-b_n^2)w_m - b_n^2 Ra_m\theta_m \\ (D^2-b_n^2)\theta_m + w_m \end{pmatrix}, \tag{3.36}$$

The interface boundary conditions for θ_f and θ_m at $z=0$ are

$$\begin{cases} \hat{d}\theta_f = \epsilon_T^2\theta_m, \quad D\theta_f = \epsilon_T D\theta_m, \qquad w_f = \hat{d}w_m, \\ (D^2+a_n^2)w_f = \frac{\hat{d}\alpha}{\sqrt{Da}}Dw_f, \\ \frac{\sigma_n}{Pr_f}Dw_f - (D^2-a_n^2)Dw_f + 2a_n^2 Dw_f = \frac{\sigma_n\epsilon_T\hat{d}^2}{\chi Pr_m}Dw_m + \frac{\hat{d}^4}{Da}Dw_m. \end{cases} \tag{3.37}$$

Throughout, the width of the free flow region is fixed at $b = 2\pi$. We also recall the following relations

$$b = \hat{d}a, \quad Ra_f = \frac{\hat{d}^4}{Da\epsilon_T^2}Ra_m, \quad Pr_f = \frac{1}{\epsilon_T}Pr_m. \tag{3.38}$$

Since the eigenvalue appears in the interface boundary condition (4.54), we adopt the Chebyshev-tau method [21] for solving the generalized eigenvalue problem (3.34)–(4.54). For the parameters that we have tested, we find that the eigenvalues are always real, which are in agreement with the results in [23].

First we examine the validity of principle of exchange of stability for generic ϵ_T, cf. Theorem 3.1 for the case of $\epsilon_T = 1$. Noting the relation (3.38), the PES condition (3.20) can be expressed in modal form

$$\begin{aligned} &\sigma_{n_c,1}(Ra_m)\begin{cases} >0, & Ra_m > Ra_m^0, \\ =0, & Ra_m = Ra_m^0, \\ <0, & Ra_m < Ra_m^0, \end{cases} \\ &\sigma_{n,k}(Ra_m^0) < 0, \quad \forall (n,k) \neq (n_c,1), \end{aligned} \tag{3.39}$$

where $Ra_m^0 := \min_n\{\text{roots of } \sigma_{n,1}(Ra_m) = 0\}$ is the critical porous Rayleigh number. In Fig. 2 we plot the modal critical Rayleigh number as a function of the height ratio $\hat{d}$ (free flow vs porous media), and the aspect ratio b, respectively while keeping other parameters fixed. It is observed that there are a finite number of $\hat{d}$ and b at which the modal neutral stability curves may intersect, indicating that two or more eigenvalues (corresponding to different n) simultaneously cross the imaginary axis as Ra_m becomes critical. Reflected on the global neutral stability curves (Fig. 3) are the discontinuities where the critical mode n_c changes value. At these discontinuities there are two (real) eigenvalues becoming critical, which are isolated degenerate cases beyond the scope of this work. Except these degenerate cases, the modal PES condition (3.39) holds true. One also observes as the height ratio of fluid over porous layer increases, transition from stability to instability happens at smaller Rayleigh number, which is consistent with the fact that fluid layer governed by the Navier-Stokes equations plays more dominating role at higher height ratio.

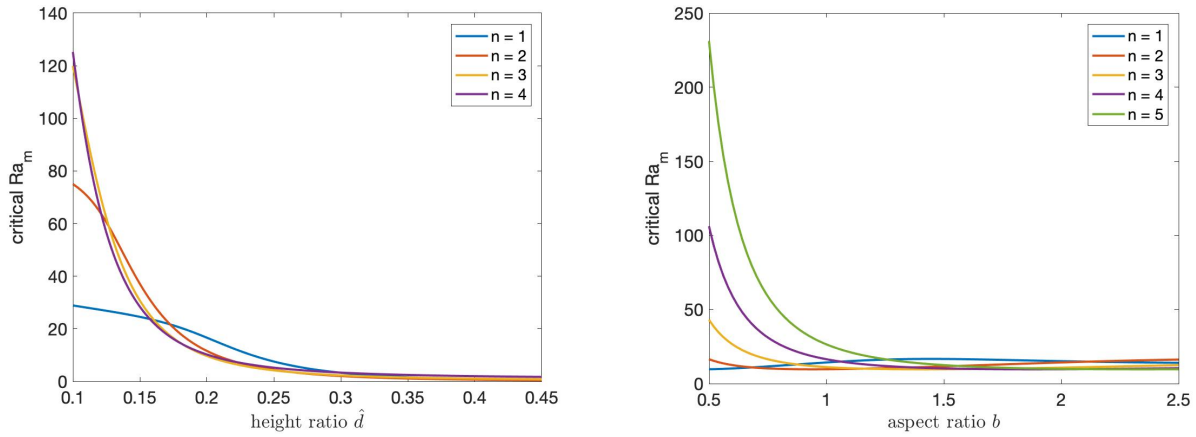

Figure 2: Plot of modal critical Rayleigh number as a function of height ratio (left) and aspect ratio (right), respectively. The parameters are: $Pr_f = 6$; $\alpha = 1$; $\rho = 10$, $\epsilon_T = 0.7$, $\chi = 0.3$, $Da = 25 \times 10^{-6}$, $b = 1.5$, $\hat{d} = 0.2$.

4 Center manifold reduction and the transition theorem

In this section we examine the stability and transition/bifurcation of the zero solution to the nonlinear system (2.9)–(2.11) by reducing the dissipative infinite-dimensional dynamical system to a finite-dimensional one (ODEs) via the center manifold reduction, cf. [15, 35, 39, 44]. Under the assumption of the PES condition (3.20), the underlying phase space can be decomposed as $\mathbf{H}_c \bigoplus \mathbf{H}_s$ with $\mathbf{H}_c$ being the center-unstable space and $\mathbf{H}_s$ being the space generated by the stable eigenfunctions associated with the eigenvalue problem (3.17)–(3.18) in the vicinity of the critical porous Rayleigh number Ra_f^0 (equivalently, Ra_m^0). The theory of dynamic system (cf. references cited earlier) implies the existence of the center-unstable invariant manifold function $\mathbf{h} : \mathbf{H_c} \to \mathbf{H_s}$ such that $\mathbf{h}(0) = D\mathbf{h}(0) = 0$, and the equivalence of dynamics (stability and transition) between the infinite-dimension dynamical system and its projection onto the center unstable space.

Because the nonlinear terms in the system are quadratic, the leading order approximation of $\mathbf{h}$ is the bilinear form

$$\mathbf{h}_2(\phi) = \frac{1}{2} D^2\mathbf{h}(0)(\phi, \phi), \quad \phi \in \mathbf{H}_c. \tag{4.40}$$

This term is determined by the so-called backward-forward procedure introduced in [12]; see also [10, Sec. 3.2]. This procedure relies on the pullback characterization of approximations to (local) invariant manifolds [12, Chap. 4]. Specifically, let ϕ be any element in H_c with proper parametrization. Then we solve the linearized equations backwards in time with initial datum ϕ at $t = 0$, and denote the corresponding solution by $\mathbf{U}^{(1)}$. Then, we solve the linearized equations forward in time by using $P_s G\big(\mathbf{U}^{(1)}, \mathbf{U}^{(1)}\big)$ as a source term, imposing that the corresponding solution $\mathbf{U}^{(2)}[\phi]$ vanishes as $t \to -\infty$. Here P_s is the projection operator onto $\mathbf{H}_s$ and G represents the nonlinear terms of the system. Note also the dependence of $\mathbf{U}^{(2)}$ on ϕ through the source term. The bilinear form $\mathbf{h}_2(\phi)$ is identified as $\mathbf{U}^{(2)}[\phi]|_{t=0}$.

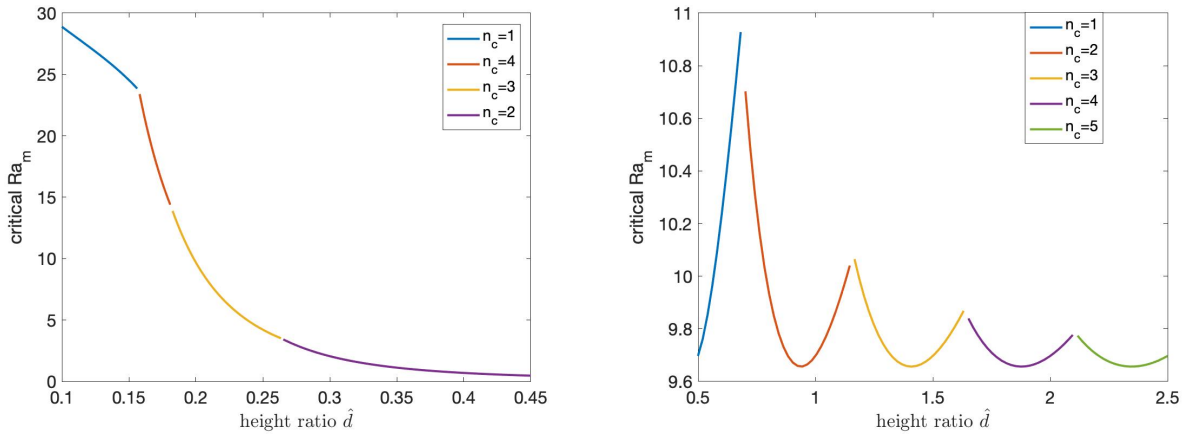

Figure 3: Neutral stability curves: critical porous Rayleigh number vs height ratio (left) and critical porous Rayleigh number vs aspect ratio (right), respectively. The parameters are: $Pr_f = 6$; $\alpha = 1$; $\rho = 10$, $\epsilon_T = 0.7$, $\chi = 0.3$, $Da = 25 \times 10^{-6}$, $b = 1.5$, $\hat{d} = 0.2$.

We assume that the modal PES condition (3.39) holds. Denote the eigenfunctions corresponding to the first eigenvalue $\sigma_1 = \sigma_{n_c,1}$ of the eigenvalue problem (3.17)-(3.18) in the vicinity of the critical Rayleigh number Ra_m^0 by

$$\psi^p = \left(\mathbf{v}_f^p, \theta_f^p, \mathbf{v}_m^p, \theta_m^p\right)^T, \quad p = n_c, \tag{4.41}$$

where

$$\begin{aligned}
&\mathbf{v}_s^p := \mathbf{V}_s^p(z)e_s^p = \left(U_s^p(z), W_s^p(z)\right)e_s^p, \quad \theta_s^p := \Theta_s^p(z)e_s^p, \quad s = f, m,\\
&e_f^p = \exp\left(ia_p x\right) = \cos a_p x + i \sin a_p x, \quad 0 \le x \le a,\\
&e_m^p = \exp\left(ib_p x\right) = \cos b_p x + i \sin b_p x, \quad 0 \le x \le b.
\end{aligned}$$

We recall that $W_s^p(z), \Theta_s^p(z)$ $(s = f, m)$ are the real eigenfunctions of the eigenvalue problem (3.34)-(4.54), and $U_f^p(z), U_m^p(z)$ are purely imaginary functions determined by integrating the divergence-free condition

$$U_f^p(z) = i\frac{DW_f^p(z)}{a_p}, \quad U_m^p(z) = i\frac{DW_m^p(z)}{b_p}.$$

Since the coefficients of the eigenvalue problem (3.17)-(3.18) are real, one thus can see that the real part and imaginary part of ψ^p are two real eigenfunctions corresponding to the first eigenvalue σ_1. Throughout we assume that the algebraic multiplicity of σ_1 equals its geometric multiplicity equal to 2, which is the general case from our numerical results in subsection 3.2. We note that the non-general case when the algebraic multiplicity of σ_1 may be 4 or greater than 4 can be treated similarly albeit more involved. For the purpose of projection, we shall also make use of the dual eigenfunction $\psi^{p*} = \left(\mathbf{v}_f^{p*}, \theta_f^{p*}, \mathbf{v}_m^{p*}, \theta_m^{p*}\right)^T$ associated with the first eigenvalue σ_1 of the adjoint eigenvalue problem. We now parameterize the center unstable space by

$$\mathbf{H}_c = \left\{y\psi^p + \overline{y\psi^p} \middle| y \in \mathbb{C}\right\}, \quad \psi^p = \psi_r^p + i\psi_i^p, \quad y = y_1 + iy_2. \tag{4.42}$$

For convenience, let ϕ_i and $\mathbf{h}_i(\phi)$ be the ith component of ϕ and $\mathbf{h}(\phi)$, respectively, , $1 \le i \le 6$, and denote

$$\phi_f = (\phi_1, \phi_2), \quad \mathbf{h}_f(\phi) = (h_1(\phi), h_2(\phi)), \quad \phi_m = (\phi_4, \phi_5), \quad \mathbf{h}_m(\phi) = (h_4(\phi), h_5(\phi)).$$

We introduce some useful identities for the center manifold reduction. Hereafter $(\cdot, \cdot)$ represents the Hermitian L^2 inner product.

Lemma 4.1. *Suppose that the PES condition (3.20) holds, and that the first eigenvalue is real of algebraic multiplicity 2 (i.e., $m^* = 2in$ (3.20)). Then the following identities hold*

$$\begin{aligned}
&\int_{\Omega_f} \overline{\theta_f^p} \cdot \overline{\theta_f^{p*}}\, dxdz = \int_{\Omega_m} \overline{\theta_m^p} \cdot \overline{\theta_m^{p*}}\, dxdz = 0,\\
&\int_{\Omega_f} \overline{\mathbf{v}_f^p} \cdot \overline{\mathbf{v}_f^{p*}}\, dxdz = \int_{\Omega_m} \overline{\mathbf{v}_m^p} \cdot \overline{\mathbf{v}_m^{p*}}\, dxdz = 0,\\
&\frac{\hat{d}}{Pr_f} \int_{\Omega_f} \mathbf{h}_f(\phi) \cdot \overline{\mathbf{v}_f^{p*}}\, dxdz + \frac{\epsilon_T \hat{d}^2}{\chi Pr_m} \int_{\Omega_m} \mathbf{h}_m(\phi) \cdot \overline{\mathbf{v}_m^{p*}}\, dxdz\\
&+ Ra_f \hat{d} \int_{\Omega_f} h_3(\phi) \cdot \overline{\theta_f^{p*}}\, dxdz + \frac{\epsilon_T^4 \varrho}{\hat{d}^2} \int_{\Omega_m} h_6(\phi) \cdot \overline{\theta_m^{p*}}\, dxdz = 0, \quad \forall \phi \in \mathbf{H}_c.
\end{aligned} \tag{4.43}$$

Proof. The first two identities are due to $\int_0^a e_f^{-2p}\, dx = \int_0^b e_m^{-2p}\, dx = 0$.

To establish the third identity, we denote the stable eigenfunctions corresponding to $\sigma_j, j = 3, 4, 5\cdots$ (counting multiplicity) of the eigenvalue problem (3.17)-(3.18) as

$$\psi_j = (\mathbf{v}_{f,j}, \theta_{f,j}, \mathbf{v}_{m,j}, \theta_{m,j}).$$

Since $\mathbf{h} : \mathbf{H}_c \to \mathbf{H}_s = (\mathbf{H}_c)^\perp$, $\mathbf{h}$ admits the following spectral expansion

$$\mathbf{h}(\phi) = \sum_{j=3}^{+\infty} a_j \psi_j, \quad \forall \phi \in \mathbf{H}_c.$$

Following the derivation of Eqs. (3.24) and (3.25) (see also Eq. (3.28)), one obtains by the adjoint eigenvalue problem

$$\begin{aligned}
&\sigma_j \hat{d} \left(\frac{1}{Pr_f} \mathbf{v}_{f,j}, \mathbf{v}_f^{p*} \right) + Ra_f \hat{d} \sigma_j \left(\theta_{f,j}, \theta_f^{p*} \right) + \frac{\sigma_j \hat{d}^2 \epsilon_T}{\chi Pr_m} \left(\mathbf{v}_{m,j}, \mathbf{v}_m^{p*} \right) + \sigma_j Ra_f \frac{\epsilon_T^4 \varrho}{\hat{d}^2} \left(\theta_{m,j}, \theta_m^{p*} \right)\\
&= -2\hat{d}(\mathbb{D}(\mathbf{v}_{f,j}), \mathbb{D}(\mathbf{v}_f^{p*})) - Ra_f \hat{d}(\nabla \theta_{f,j}, \nabla \theta_f^{p*}) - \frac{\hat{d}^4}{Da}(\mathbf{v}_{m,j}, \mathbf{v}_m^{p*}) - Ra_f \epsilon_T^3 (\nabla \theta_{m,j}, \nabla \theta_m^p)\\
&\quad + \hat{d} Ra_f (\theta_{f,j}, w_f^{p*}) + \hat{d} Ra_f (w_{f,j}, \theta_f^{p*}) + Ra_f \epsilon_T^2 (\theta_{m,j}, w_m^{p*}) + Ra_f \epsilon_T^3 (w_{m,j}, \theta_m^{p*})\\
&\quad - 2\frac{\hat{d}^2 \alpha}{\sqrt{Da}} \sum_{s=1}^{2} \int_{\Gamma_i} (\mathbf{v}_{f,j} \cdot \tau_s)(\overline{\mathbf{v}_f^{p*}} \cdot \tau_s)\, d\Gamma_i\\
&= \overline{\sigma_1} \hat{d} \left(\frac{1}{Pr_f} \mathbf{v}_{f,j}, \mathbf{v}_f^{p*} \right) + Ra_f \hat{d} \overline{\sigma_1} \left(\theta_{f,j}, \theta_f^{p*} \right) + \frac{\overline{\sigma_1} \hat{d}^2 \epsilon_T}{\chi Pr_m} \left(\mathbf{v}_{m,j}, \mathbf{v}_m^{p*} \right) + \overline{\sigma_1} Ra_f \frac{\epsilon_T^4 \varrho}{\hat{d}^2} \left(\theta_{m,j}, \theta_m^{p*} \right).
\end{aligned}$$

Hence

$$\hat{d} \left(\frac{1}{Pr_f} \mathbf{v}_{f,j}, \mathbf{v}_f^{p*} \right) + Ra_f \hat{d} \left(\theta_{f,j}, \theta_f^{p*} \right) + \frac{\hat{d}^2 \epsilon_T}{\chi Pr_m} \left(\mathbf{v}_{m,j}, \mathbf{v}_m^{p*} \right) + Ra_f \frac{\epsilon_T^4 \varrho}{\hat{d}^2} \left(\theta_{m,j}, \theta_m^{p*} \right) = 0, \quad j = 3, 4, \cdots$$

This establishes the third identity. □

Likewise, the following identities can be readily verified.

Lemma 4.2. *Under the same condition as Lemma 4.1 the following identities hold:*

$$\begin{aligned}
&\int_{\Omega_f}\Big((\mathbf{v}_f^p\cdot\nabla)\mathbf{v}_f^p\Big)\cdot\overline{\mathbf{v}_f^{p*}}\,dxdz=\int_{\Omega_f}\Big((\mathbf{v}_f^p\cdot\nabla)\overline{\mathbf{v}_f^p}\Big)\cdot\overline{\mathbf{v}_f^{p*}}\,dxdz=0,\\
&\int_{\Omega_f}\Big((\overline{\mathbf{v}_f^p}\cdot\nabla)\mathbf{v}_f^p\Big)\cdot\overline{\mathbf{v}_f^{p*}}\,dxdz=\int_{\Omega_f}\Big((\overline{\mathbf{v}_f^p}\cdot\nabla)\overline{\mathbf{v}_f^p}\Big)\cdot\overline{\mathbf{v}_f^{p*}}\,dxdz=0,
\end{aligned}\tag{4.44}$$

$$\begin{aligned}
&\int_{\Omega_s}\Big((\mathbf{v}_s^{(p)}\cdot\nabla)\theta_s^p\Big)\cdot\overline{\theta_s^{p*}}\,dxdz=\int_{\Omega_s}\Big((\mathbf{v}_f^{(p)}\cdot\nabla)\overline{\theta_s^p}\Big)\cdot\overline{\theta_s^{p*}}\,dxdz=0,\\
&\int_{\Omega_s}\Big((\overline{\mathbf{v}_s^{(p)}}\cdot\nabla)\theta_s^p\Big)\cdot\overline{\theta_s^{p*}}\,dxdz=\int_{\Omega_s}\Big((\overline{\mathbf{v}_s^{(p)}}\cdot\nabla)\overline{\theta_s^p}\Big)\cdot\overline{\theta_s^{p*}}\,dxdz=0,
\end{aligned}\tag{4.45}$$

where $s=f,m$.

According to theory of dissipative dynamical system [**?**, 15, 35, 44], one obtains the following equivalent (in terms of stability and transition) reduced equation.

Lemma 4.3. *Assume that the PES condition (3.20) holds, and that the first eigenvalue is real of algebraic multiplicity 2 (i.e., $m^*=2$ in (3.20)). Then, the transition and stability of the zero steady state solution to the equations (2.9)–(2.11) in the vicinity of the critical Rayleigh number Ra_f^0 and for any sufficiently small initial condition are equivalent to those of the zero solution of the equation*

$$\frac{d\eta}{dt}=\sigma_1\eta+P\eta|\eta|^2+o(|\eta|^3),\tag{4.46}$$

where η is a complex-valued function and $P\in\mathbb{R}$ is the transition number defined in (4.65) and (4.67).

Proof. Following the procedure outlined above, we first derive the leading-order approximation of the center manifold function, then we project the infinite-dimensional dynamical system onto the center unstable space. We divide the derivation into three steps.

Step 1: The second-order approximation of the center manifold function.
We follow the backward-forward procedure [12] to derive the second-order approximation of the center manifold function $\mathbf{h}_2$, cf. (4.40).

In the neighborhood of the critical Rayleigh number Ra_f^0, for any $\phi\in\mathbf{H}_c=\{y\psi^p+\overline{y\psi^p}|y\in\mathbb{C}\}$, we first solve backwards in time the linear problem (3.13)-(3.16) projected onto $\mathbf{H}_c$ with the initial condition ϕ, i.e.,

$$\mathbf{v}_s^{(1)}|_{t=0}=y\mathbf{V}_s^p(z)e_s^p+\overline{y\mathbf{V}_s^p(z)e_s^p},\quad \theta_s^{(2)}|_{t=0}=y\Theta_s^p(z)e_s^p+\overline{y\Theta_s^p(z)e_s^p},\quad s=f,m.$$

The linear system of ODEs admits a unique solution for all time. In light of the eigenvalue problem (3.17)-(3.18), the solution takes the form of

$$\begin{aligned}
\mathbf{v}_s^{(1)}&=y\mathbf{v}_s^p(z)e^{\sigma_1 t}e_s^p+\overline{y\mathbf{v}_s^p(z)e^{\sigma_1 t}e_s^p},\\
\theta_s^{(1)}&=y\theta_s^p(z)e^{\sigma_1 t}e_s^p+\overline{y\theta_s^p(z)e^{\sigma_1 t}e_s^p},\quad s=f,m.
\end{aligned}\tag{4.47}$$

Next we consider the linear problem forced by $(\mathbf{v}_s^{(1)}, \theta_s^{(1)}), s = f, m$, via the nonlinear terms

$$\begin{cases} \frac{1}{Pr_f}\frac{\partial \mathbf{v}_f}{\partial t} = 2\nabla\cdot\mathbb{D}(\mathbf{v}_f) - \nabla\pi_f + Ra_f\theta_f\mathbf{k} - (\mathbf{v}_f^{(1)}\cdot\nabla)\mathbf{v}_f^{(1)}, \quad \text{in } \Omega_f, \\ \nabla\cdot\mathbf{v}_f = 0, \quad \text{in } \Omega_f, \\ \frac{\partial\theta_f}{\partial t} = \Delta\theta_f + w_f - Pr_f\mathbf{v}_f^{(1)}\cdot\nabla\theta_f^{(1)}, \quad \text{in } \Omega_f, \\ \theta_f = 0, \quad \mathbf{v}_f = 0, \quad \text{at } z = 1, \end{cases} \tag{4.48}$$

coupled with

$$\begin{cases} \frac{\epsilon_T Da}{\hat{d}^2\chi Pr_m}\frac{\partial \mathbf{v}_m}{\partial t} + \mathbf{v}_m = -Da\nabla\pi_m + Ra_m\theta_m\mathbf{k}, \quad \text{in } \Omega_m, \\ \nabla\cdot\mathbf{u}_m = 0, \quad \text{in } \Omega_m, \\ \frac{\epsilon_T\varrho}{\hat{d}^2}\frac{\partial\theta_m}{\partial t} = \Delta\theta_m + w_m - Pr_m\mathbf{v}_m^{(1)}\cdot\nabla\theta_m^{(1)}, \quad \text{in } \Omega_m, \\ \theta_m = 0, \quad w_m = 0, \quad \text{at } z = -1, \end{cases} \tag{4.49}$$

subject to the interface conditions

$$\begin{cases} \hat{d}\theta_f = \epsilon_T^2\theta_m, \quad \frac{\partial\theta_f}{\partial z} = \epsilon_T\frac{\partial\theta_m}{\partial z}, \quad w_f = \hat{d}w_m, \quad \text{on } z = 0, \\ \frac{\partial u_f}{\partial z} + \frac{\partial w_f}{\partial x} = \frac{\hat{d}\alpha}{\sqrt{Da}}u_f, \quad \text{on } z = 0, \\ \pi_f - 2\frac{\partial w_f}{\partial z} + \frac{1}{2}\left(\left(u_f^{(1)}\right)^2 + \left(w_f^{(1)}\right)^2\right) = \hat{d}^2\pi_m, \quad \text{on } z = 0. \end{cases} \tag{4.50}$$

We integrate the linear system projected onto the stable space $\mathbf{H}_s$ forward in-time with the condition

$$\lim_{t\to-\infty}\mathbf{v}_s^{(2)} = \lim_{t\to-\infty}\theta_s^{(2)} = 0, \quad s = f, m.$$

The solution form (4.47) suggests the following ansatz, for $t < 0$

$$\begin{aligned} \mathbf{v}_s^{(2)} &= |y|^2\tilde{\mathbf{v}}_s^{(p,0)}(z)e^{2Re\sigma_1 t} + y^2\tilde{\mathbf{v}}_s^{(p,1)}(z)e^{2\sigma_1 t}e_s^{2p} + \overline{y}^2\tilde{\mathbf{v}}_s^{(p,2)}(z)e^{2\overline{\sigma_1}t}e_s^{-2p}, \\ \theta_s^{(2)} &= |y|^2\tilde{\theta}_s^{(p,0)}(z)e^{2Re\sigma_1 t} + y^2\tilde{\theta}_s^{(p,1)}(z)e^{2\sigma_1 t}e_s^{2p} + \overline{y}^2\tilde{\theta}_s^{(p,2)}(z)e^{2\overline{\sigma_1}t}e_s^{-2p}, \qquad s = f, m. \end{aligned} \tag{4.51}$$

One can derive the equations satisfied by $(\tilde{\mathbf{v}}_s^{(p,i)}, \tilde{\theta}_s^{(p,i)}), i = 0, 1, 2, s = f, m$ by substituting the preceding expressions into the coupled system (4.48)-(4.50), comparing the modes, and also eliminating the pressure. In particular, it follows from the divergence-free condition and the boundary condition that

$$\tilde{w}_s^{(p,0)}(z) = 0, \quad s = f, m,$$

which combining with the governing equation implies

$$\tilde{u}_s^{(p,0)}(z) = 0, \quad s = f, m.$$

In addition, $\tilde{\theta}_s^{(p,0)}(z)$ $(s = f, m)$ solve the steady equations

$$\begin{cases} 2Re\sigma_1\tilde{\theta}_f^{(p,0)}(z) = D^2\tilde{\theta}_f^{(p,0)}(z) - 2Pr_f\left(w_f^p(z)D\theta_f^p(z) + Dw_f^p(z)\theta_f^p(z)\right), \quad z \in (0,1), \\ 2\frac{\epsilon_T\varrho}{\hat{d}^2}Re\sigma_1\tilde{\theta}_m^{(p,0)}(z) = D^2\tilde{\theta}_m^{(p,0)}(z) - 2Pr_m\left(w_m^p(z)D\theta_m^p(z) + Dw_m^p(z)\theta_m^p(z)\right), \quad z \in (-1,0), \\ \tilde{\theta}_f^{(p,0)}(1) = 0, \quad \tilde{\theta}_m^{(p,0)}(-1) = 0, \end{cases}$$

subject to the interface boundary conditions

$$\begin{cases} \hat{d}\tilde{\theta}_f^{(p,0)}(0) = \epsilon_T^2 \tilde{\theta}_m^{(p,0)}(0), \\ \frac{d\tilde{\theta}_f^{(p,0)}}{dz}(0) = \epsilon_T \frac{d\tilde{\theta}_m^{(p,0)}}{dz}(0). \end{cases} \tag{4.52}$$

Likewise, one can verify that $(\tilde{w}_s^{(p,1)}(z), \tilde{\theta}_s^{(p,1)}(z)), s = f, m$, satisfy

$$\begin{cases} 2\sigma_1 \mathcal{A}_{2p}^f \psi_f^{(p,1)} = \mathcal{L}_{2p}^f \psi_f^{(p,1)} + \mathcal{F}_p^f \psi_f^p, \quad z \in (0,1), \\ 2\sigma_1 \mathcal{A}_{2p}^m \psi_m^{(p,1)} = \mathcal{L}_{2p}^m \psi_m^{(p,1)} + \mathcal{F}_p^m \psi_m^p, \quad z \in (-1,0), \\ w_f^{(p,1)} = Dw_f^{(p,1)} = \theta_f^{(p,1)} = 0, \quad z = 1, \\ w_m^{(p,1)} = \theta_m^{(p,1)} = 0, \quad z = -1, \end{cases} \tag{4.53}$$

where

$$\begin{aligned} &\psi_s^{(p,1)} = (w_s^{(p,1)}(z), \theta_s^{(p,1)}(z)), \quad s = f, m, \\ &\mathcal{F}_p^f \psi_f^p = \begin{pmatrix} a_{2p} i D \mathcal{G}_p^f u_f^p + 4a_p^2 \mathcal{G}_p^f w_f^p \\ -Pr_f \mathcal{G}_p^f \theta_f^p \end{pmatrix}, \quad \mathcal{F}_p^m \psi_m^p = \begin{pmatrix} 0 \\ -Pr_m \mathcal{G}_p^m \theta_m^p \end{pmatrix}, \end{aligned}$$

with

$$\begin{aligned} \mathcal{G}_p^f g(z) =& a_p i \left(u_f^p(z) g(z) \right) + \left(w_f^p(z) Dg(z) \right), \\ \mathcal{G}_p^m g(z) =& b_p i \left(u_m^p(z) g(z) \right) + \left(w_m^p(z) Dg(z) \right). \end{aligned}$$

The interface conditions at $z = 0$ are

$$\begin{cases} \hat{d}\theta_f^{(p,1)} = \epsilon_T^2 \theta_m^{(p,1)}, \\ D\theta_f^{(p,1)} = \epsilon_T D\theta_m^{(p,1)}, \\ w_f^{(p,1)} = \hat{d} w_m^{(p,1)}, \\ (D^2 + a_{2p}^2) w_f^{(p,1)} = \frac{\hat{d}\alpha}{\sqrt{Da}} Dw_f^{(p,1)}, \\ \frac{2\sigma_1}{Pr_f} Dw_f^{(p,1)} - (D^2 - a_{2p}^2) Dw_f^{(p,1)} + 2a_{2p}^2 Dw_f^{(p,1)} \\ - \frac{2\epsilon_T \sigma_1 \hat{d}^2}{\chi Pr_m} Dw_m^{(p,1)} - \frac{\hat{d}^4}{Da} Dw_m^{(p,1)} = -\frac{a_{2p}^2}{2} \left(\left(u_f^p \right)^2 + \left(w_f^p \right)^2 \right). \end{cases} \tag{4.54}$$

The horizontal component of the velocity can be recovered from the divergence-free condition, for instance

$$i a_{2p} \tilde{u}_m^{(p,1)} + D\tilde{w}_m^{(p,1)} = 0.$$

One also observes that

$$\tilde{\mathbf{v}}_s^{(p,2)}(z) = \overline{\tilde{\mathbf{v}}_s^{(p,1)}(z)}, \quad \tilde{\theta}_s^{(p,2)}(z) = \overline{\tilde{\theta}_s^{(p,1)}(z)}, \quad s = f, m.$$

Then, the second-order approximation of the center manifold function is given by

$$\mathbf{h}_2(\phi) = \left(\mathbf{v}_f^{(2)}, \theta_f^{(2)}, \mathbf{v}_m^{(2)}, \theta_m^{(2)} \right)^T |_{t=0}, \tag{4.55}$$

where $(\mathbf{v}_s^{(2)}, \theta_s^{(2)}), s = f, m$ are defined in (4.51).

Step 2: Projection onto the center space.

We make use of the dual eigenfunction $\psi^\star$ and the approximation of the center manifold function to reduce the infinite-dimensional dynamical system to a finite-dimensional one. By integration by parts, one deduces from the equations (2.9)-(2.10) that

$$\begin{aligned}
\frac{1}{Pr_f}\left(\frac{\partial \mathbf{v}_f}{\partial t}, \mathbf{v}_f^{p*}\right) &= -2\big(\mathbb{D}(\mathbf{v}_f), \mathbb{D}(\mathbf{v}_f^{p*})\big) + (Ra_f\theta_f, \mathbf{v}_f^{p*}) \\
&\quad - 2\sum_{s=1}^{2}\int_{\Gamma_i} \tau_s \cdot \mathbb{D}(\mathbf{v}_f)\mathbf{n}(\overline{\mathbf{v}_f^{p*}} \cdot \tau_s)\, d\Gamma_i \\
&\quad - \int_{\Gamma_i}\left(2\frac{\partial w_f}{\partial z} - \pi_f\right)(\overline{\mathbf{v}_f^{p*}} \cdot \mathbf{n})\, d\Gamma_i - \left((\mathbf{v}_f \cdot \nabla)\mathbf{v}_f, \mathbf{v}_f^{p*}\right),
\end{aligned} \tag{4.56}$$

$$\begin{aligned}
\frac{\epsilon_T}{\hat{d}^2\chi Pr_m}\left(\frac{\partial \mathbf{v}_m}{\partial t}, \mathbf{v}_m^{p*}\right) &= -\frac{1}{Da}(\mathbf{v}_m, \mathbf{v}_m^{p*}) - (\nabla\pi_m, \mathbf{v}_m^{p*}) + \frac{Ra_m}{Da}(\theta_m, w_m^{p*}) \\
&= -\frac{1}{Da}(\mathbf{v}_m, \mathbf{v}_m^{p*}) - \int_{\Gamma_i}\pi_m(\overline{\mathbf{v}_m^{p*}} \cdot \mathbf{n})\, d\Gamma_i + \frac{Ra_m}{Da}(\theta_m, w_m^{p*}),
\end{aligned} \tag{4.57}$$

$$\begin{aligned}
\left(\frac{\partial \theta_f}{\partial t}, \theta_f^{p*}\right) &= -(\nabla\theta_f, \nabla\theta_f^{p*}) - \int_{\Gamma_i}\theta_f(\nabla\overline{\theta_f^{p*}} \cdot \mathbf{n})\, d\Gamma_i + (w_f, \theta_f^{p*}) \\
&\quad - \left((\mathbf{v}_f \cdot \nabla)\theta_f, \theta_f^{p*}\right),
\end{aligned} \tag{4.58}$$

$$\begin{aligned}
\frac{\epsilon_T\varrho}{\hat{d}^2}\left(\frac{\partial \theta_m}{\partial t}, \theta_m^{p*}\right) &= -(\nabla\theta_m, \nabla\theta_m^{p*}) - \int_{\Gamma_i}\theta_m(\nabla\overline{\theta_m^{p*}} \cdot \mathbf{n})\, d\Gamma_i + (w_m, \theta_m^{p*}) \\
&\quad - ((\mathbf{v}_m \cdot \nabla)\theta_m, \theta_m^{p*}).
\end{aligned} \tag{4.59}$$

Furthermore, $\hat{d} \times$ (4.56) $+ \hat{d}^4 \times$ (4.57) $+ Ra_f\hat{d} \times$ (4.58) $+ Ra_f\epsilon^3 \times$ (4.59) gives

$$\begin{aligned}
&\frac{\hat{d}}{Pr_f}\left(\frac{\partial \mathbf{v}_f}{\partial t}, \mathbf{v}_f^{p*}\right) + \frac{\epsilon_T\hat{d}^2}{\chi Pr_m}\left(\frac{\partial \mathbf{v}_m}{\partial t}, \mathbf{v}_m^{p*}\right) + Ra_f\hat{d}\left(\frac{\partial \theta_f}{\partial t}, \theta_f^{p*}\right) + Ra_f\frac{\epsilon_T^4\varrho}{\hat{d}^2}\left(\frac{\partial \theta_m}{\partial t}, \theta_m^{p*}\right) \\
&= -2\hat{d}\big(\mathbb{D}(\mathbf{v}_f), \mathbb{D}(\mathbf{v}_f^{p*})\big) + \hat{d}(Ra_f\theta_f, w^{p*}) - \frac{\hat{d}^4}{Da}(\mathbf{v}_m, \mathbf{v}_m^{p*}) + Ra_f\epsilon_T^2(\theta_m, w_m^{p*}) \\
&\quad - Ra_f\hat{d}(\nabla\theta_f, \nabla\theta_f^{p*}) + \hat{d}Ra_f(w_f, \theta_f^{p*}) - Ra_f\epsilon_T^3(\nabla\theta_m, \nabla\theta_m^{p*}) + Ra_f\epsilon_T^3(w_m, \theta_m^{p*}) \\
&\quad - 2\frac{\hat{d}^2\alpha}{\sqrt{Da}}\sum_{s=1}^{2}\int_{\Gamma_i}(\mathbf{v}_f \cdot \tau_s)(\overline{\mathbf{v}_f^{p*}} \cdot \tau_s)\, d\Gamma_i - \hat{d}\left((\mathbf{v}_f \cdot \nabla)\mathbf{v}_f, \mathbf{v}_f^{p*}\right) \\
&\quad - Pr_fRa_f\hat{d}\left((\mathbf{v}_f \cdot \nabla)\theta_f, \theta_f^{p*}\right) - Pr_mRa_f\epsilon_T^3\left((\mathbf{v}_m \cdot \nabla)\theta_m, \theta_m^{p*}\right) \\
&\quad - \frac{\hat{d}}{2}\int_{\Gamma_i}|\mathbf{v}_f|^2(\overline{\mathbf{v}_f^{p*}} \cdot \mathbf{n})\, d\Gamma_i.
\end{aligned} \tag{4.60}$$

In the vicinity of the critical Rayleigh number Ra_f^0, we write

$$(\mathbf{v}_f, \theta_f, \mathbf{v}_m, \theta_m)^T = \phi + \mathbf{h}(\phi),$$

where $\phi \in \mathbf{H}_c$ has the representation

$$\phi = \eta(t)\psi^p + \overline{\eta(t)\psi^p}, \quad \psi^p = (\psi_f^p, \psi_m^p) = \left(\mathbf{v}_f^p, \theta_f^p, \mathbf{v}_m^p, \theta_m^p\right)^T.$$

We recall that ψ^p is the eigenfunction corresponding to the first critical eigenvalue $\sigma_1 = \sigma_2$, and that the center manifold function $\mathbf{h}$ admits the expansion

$$\mathbf{h}(\phi) = \mathbf{h}_2(\phi) + o(|\eta|^2), \tag{4.61}$$

with the second-order approximation given by Eq. (4.55). With the help of the identities in Lemma 4.1 and 4.2 the equation (4.60) becomes

$$\begin{aligned}
\frac{d\eta}{dt}Q =& -2\hat{d}\eta\big(\mathbb{D}(\mathbf{v}_f^p), \mathbb{D}(\mathbf{v}_f^{p*})\big) + \hat{d}\eta(Ra_f\theta_f^p, w^{p*}) - \frac{\hat{d}^4\eta}{Da}(\mathbf{v}_m^p, \mathbf{v}_m^{p*}) \\
&+ Ra_f\epsilon_T^2\eta(\theta_m^p, w_m^{p*}) - Ra_f\hat{d}\eta(\nabla\theta_f^p, \nabla\theta_f^{p*}) + \hat{d}Ra_f\eta(w_f^p, \theta_f^{p*}) \\
&- Ra_f\eta\epsilon_T^3(\nabla\theta_m^p, \nabla\theta_m^{p*}) + Ra_f\epsilon_T^3\eta(w_m^p, \theta_m^{p*}) \\
&- 2\eta\frac{\hat{d}^2\alpha}{\sqrt{Da}}\sum_{s=1}^{2}\int_{\Gamma_i}(\mathbf{v}_f^p\cdot\tau_s)(\overline{\mathbf{v}_f^{p*}}\cdot\tau_s)\,d\Gamma_i - \hat{d}\left((\mathbf{v}_f\cdot\nabla)\mathbf{v}_f, \mathbf{v}_f^{p*}\right) \\
&- Pr_fRa_f\hat{d}\left((\mathbf{v}_f\cdot\nabla)\theta_f, \theta_f^{p*}\right) - Pr_mRa_f\epsilon_T^3\left((\mathbf{v}_m\cdot\nabla)\theta_m, \theta_m^{p*}\right) \\
&- \frac{\hat{d}}{2}\int_{\Gamma_i}|\mathbf{v}_f|^2(\overline{\mathbf{v}_f^{p*}}\cdot\mathbf{n})\,d\Gamma_i.
\end{aligned} \tag{4.62}$$

where

$$Q = \frac{\hat{d}}{Pr_f}\left(\mathbf{v}_f^p, \mathbf{v}_f^{p*}\right) + \frac{\epsilon_T\hat{d}^2}{\chi Pr_m}\left(\mathbf{v}_m^p, \mathbf{v}_m^{p*}\right) + Ra_f\hat{d}\left(\theta_f^p, \theta_f^{p*}\right) + Ra_f\frac{\epsilon_T^4\varrho}{\hat{d}^2}\left(\theta_m^p, \theta_m^{p*}\right). \tag{4.63}$$

For the linear terms in (4.62), replacing $\left(\overline{\mathbf{v}_f}, \overline{\theta_f}, \overline{\mathbf{v}_m}, \overline{\theta_m}\right)$ by $\left(\overline{\mathbf{v}_f^{p*}}, \overline{\theta_f^{p*}}, \overline{\mathbf{v}_m^{p*}}, \overline{\theta_m^{p*}}\right)$ in (3.25), in light of the identity (3.24), one derives

$$\begin{aligned}
&-2\hat{d}\eta\big(\mathbb{D}(\mathbf{v}_f^p), \mathbb{D}(\mathbf{v}_f^{p*})\big) + \hat{d}\eta(Ra_f\theta_f^p, w^{p*}) - \frac{\hat{d}^4y}{Da}(\mathbf{v}_m^p, \mathbf{v}_m^{p*}) + Ra_f\epsilon_T^2\eta(\theta_m^p, w_m^{p*}) \\
&- Ra_f\hat{d}y(\nabla\theta_f^p, \nabla\theta_f^{p*}) + \hat{d}Ra_f\eta(w_f^p, \theta_f^{p*}) - Ra_f\eta\epsilon_T^3(\nabla\theta_m^p, \nabla\theta_m^{p*}) + Ra_f\epsilon_T^3\eta(w_m^p, \theta_m^{p*}) \\
&- 2\eta\frac{\hat{d}^2\alpha}{\sqrt{Da}}\sum_{s=1}^{2}\int_{\Gamma_i}(\mathbf{v}_f^p\cdot\tau_s)(\overline{\mathbf{v}_f^{p*}}\cdot\tau_s)\,d\Gamma_i = \sigma_1\eta Q.
\end{aligned} \tag{4.64}$$

For the nonlinear interactions, we derive by the identities in Lemma 4.2 and the definition of the second-order approximation of the center manifold function (**??**),

$$\begin{aligned}
&\hat{d}\left((\mathbf{v}_f\cdot\nabla)\mathbf{v}_f, \mathbf{v}_f^{p*}\right) - Pr_fRa_f\hat{d}\left((\mathbf{v}_f\cdot\nabla)\theta_f, \theta_f^{p*}\right) \\
&- Pr_mRa_f\epsilon_T^3\left((\mathbf{v}_m\cdot\nabla)\theta_m, \theta_m^{p*}\right) - \frac{\hat{d}}{2}\int_{\Gamma_i}|\mathbf{v}_f|^2(\overline{\mathbf{v}_f^{p*}}\cdot\mathbf{n})\,d\Gamma_i \\
&= -\hat{d}\left((\phi_f\cdot\nabla)h_f^2, \mathbf{v}_f^{p*}\right) - \hat{d}\left((\mathbf{h}_f^2\cdot\nabla)\phi_f, \mathbf{v}_f^{p*}\right) - Pr_fRa_f\hat{d}\left((\phi_f\cdot\nabla)h_3^2, \theta_f^{p*}\right) \\
&\quad - Pr_fRa_f\hat{d}\left((\mathbf{h}_f^2\cdot\nabla)\phi_3, \theta_f^{p*}\right) - Pr_mRa_f\epsilon_T^3\left((\phi_m\cdot\nabla)h_6^2, \theta_m^{p*}\right) \\
&\quad - Pr_mRa_f\epsilon_T^3\left((\mathbf{h}_m^2\cdot\nabla)\phi_6, \theta_m^{p*}\right) - \hat{d}|\eta|^2\eta\int_{\Gamma_i}\left(\overline{\mathbf{V}_f^p(0)}\cdot\tilde{\mathbf{v}}_f^{(p,1)}(0)\right)W_f^{p*}(0)\,d\Gamma_i + o(|\eta|^3) \\
&:= R_3(\eta) + o(|\eta|^3),
\end{aligned}$$

where $R_3(\eta)$ comprise the cubic terms of η that will be explicitly calculated in step 3. Note that $Q \neq 0$. Hence, Eq. (4.60) is reduced to the low-dimensional system

$$\frac{d\eta}{dt} = \sigma_1 \eta + \frac{R_3(\eta)}{Q} + o(|\eta|^3). \tag{4.65}$$

Step 3: Calculations of the coefficients in the reduced equation.
For the convenience of computing $R_3(\eta)$ we introduce some new notations

$$\begin{aligned}
&\eta_1 = \eta, \quad \eta_2 = \overline{\eta}, \quad \psi_1 = \psi^p, \quad \psi_2 = \overline{\psi^p},\\
&\psi_{1,1} = \mathbf{v}_f^p, \quad \psi_{1,2} = \theta_f^p, \quad \psi_{1,3} = \mathbf{v}_m^p, \quad \psi_{1,4} = \theta_m^p,\\
&\psi_{2,1} = \overline{\mathbf{v}_f^p}, \quad \psi_{2,2} = \overline{\theta_f^p}, \quad \psi_{2,3} = \overline{\mathbf{v}_m^p}, \quad \psi_{2,4} = \overline{\theta_m^p},\\
&\mathbf{v}_s^{(2,12)} = \mathbf{v}_s^{(2,21)} = \tilde{\mathbf{v}}_s^{(p,0)}(z)/2 = 0,\\
&\theta_s^{(2,12)} = \theta_s^{(2,21)} = \tilde{\theta}_s^{(p,0)}(z)/2,\\
&\mathbf{v}_s^{(2,11)} = \tilde{\mathbf{v}}_s^{(p,1)}(z)e_s^{2p}, \quad \mathbf{v}_s^{(2,22)} = \tilde{\mathbf{v}}_s^{(p,2)}(z)e_s^{-2p},\\
&\theta_s^{(2,11)} = \tilde{\theta}_s^{(p,1)}(z)e_s^{2p}, \quad \theta_s^{(2,22)} = \tilde{\theta}_s^{(p,2)}(z)e_s^{-2p}, \quad s = f, m.
\end{aligned} \tag{4.66}$$

Then the second order term of the center manifold function $\mathbf{h}_2(\phi)$ can be written as

$$\mathbf{h}^2(\phi) = \sum_{s=1}^{2}\sum_{k=1}^{2} \eta_s \eta_k \begin{pmatrix} \mathbf{v}_f^{(2,sk)} \\ \theta_f^{(2,sk)} \\ \mathbf{v}_m^{(2,sk)} \\ \theta_m^{(2,sk)} \end{pmatrix}$$

Hence

$$R_3(y) = \sum_{s=1}^{2}\sum_{k=1}^{2}\sum_{l=1}^{2} g_{skl}\eta_s\eta_k\eta_l,$$

with

$$\begin{aligned}
g_{skl} = &- \hat{d}\left((\psi_{l,1}\cdot\nabla)\mathbf{v}_f^{2,sk}, \mathbf{v}_f^{p*}\right) - \hat{d}\left((\mathbf{v}_f^{2,sk}\cdot\nabla)\psi_{l,1}, \mathbf{v}_f^{p*}\right)\\
&- Pr_f Ra_f \hat{d}\left((\psi_{l,1}\cdot\nabla)\theta_f^{2,sk}, \theta_f^{p*}\right) - Pr_f Ra_f \hat{d}\left((\mathbf{v}_f^{2,sk}\cdot\nabla)\psi_{l,2}, \theta_f^{p*}\right)\\
&- Pr_m Ra_f \epsilon_T^3\left((\psi_{l,3}\cdot\nabla)\theta_m^{2,sk}, \theta_m^{p*}\right) - Pr_m Ra_f \epsilon_T^3\left((\mathbf{v}_m^{2,sk}\cdot\nabla)\psi_{l,4}, \theta_m^{p*}\right)\\
&- \hat{d}\int_{\Gamma_i} (\psi_{l,1}\cdot\mathbf{v}_f^{2,sk})(\overline{\mathbf{v}_f^{p*}}\cdot\mathbf{n})\, d\Gamma_i.
\end{aligned}$$

Noting that $\mathbf{v}_s^{(2,12)} = \mathbf{v}_s^{(2,21)} = 0$, we infer that

$$g_{12l} = g_{21l} = - Pr_f Ra_f \hat{d}\left((\psi_{l,1}\cdot\nabla)\theta_f^{2,12}, \theta_f^{p*}\right) - Pr_m Ra_f \epsilon_T^3\left((\psi_{l,3}\cdot\nabla)\theta_m^{2,12}, \theta_m^{p*}\right),$$

which has the integral factor

$$\exp\big(2p_l - 2p)\pi/ax\big) \quad \text{or} \quad \exp\big(2p_l - 2p)\pi/bx\big),$$

Since

$$p_1 = p, \quad p_2 = -p,$$

one obtains

$$g_{122} = g_{212} = 0.$$

Likewise,

$$g_{111} = g_{222} = g_{221} = 0.$$

Denoting

$$G = g_{121} + g_{211} + g_{112}, \tag{4.67}$$

then the reduced equation (4.65) becomes

$$\frac{d\eta}{dt} = \sigma_1\eta + P\eta|\eta|^2 + o(|\eta|^3), \quad P = \frac{G}{Q} \in \mathbb{R}. \tag{4.68}$$

The proof is complete. □

As is expected, the reduced equation (4.68) takes the same form as the reduced one for the classical Rayleigh-Bénard problem, cf. equation (5.17) in [22]. As a result of Lemma 4.3, following the same argument as in [22] (Theorem 5.1) one can deduce the following transition theorem, see also [35] (Theorem 2.1.3 and 2.2.2).

Theorem 4.1. *Assume that the PES condition (3.20) holds, and that the first eigenvalue is real of algebraic multiplicity 2 (i.e., $m^* = 2$ in (3.20)). The following assertions hold:*

(1) *For $Ra_f < Ra_f^0$, the zero steady state solution of the perturbed system (2.9)-(2.11) is locally asymptotically stable.*

(2) *If the transition number $P < 0$, the system (2.9)-(2.11) undergoes a continuous type transition at $Ra_f = Ra_f^0$ in which the zero steady state solution bifurcates to a local attractor Σ_{Ra_f} for $Ra_f > Ra_f^0$, homeomorphic to the unit circle $\mathcal{S}^1$, with the following approximation*

$$\Sigma_{Ra_f} = \Big\{ x\,\mathrm{Re}(\psi^p) + y\,\mathrm{Im}(\psi^p) \mid x^2 + y^2 = -\frac{\sigma_1}{P} \Big\} + o\Big(\sqrt{\frac{\sigma_1}{|P|}}\Big). \tag{4.69}$$

The attractor $\Sigma_{\mathbb{R}}$ attracts $\mathcal{H} \setminus \Gamma$, where Γ is the stable manifold of 0 with codimension 2, and $\mathcal{H} \subset \mathbf{Y}$ is a open set containing 0;

(3) *If the transition number $P > 0$, the system (2.9)-(2.11) undergoes a jump transition at $Ra_f = Ra_f^0$. More precisely, there exists an open U of 0 in $\mathbf{Y}$ such that for any initial condition $\psi_0 = (\mathbf{v}_(x,z,0), \theta_(x,z,0), \mathbf{v}_m(x,z,0), \theta_m(x,z,0)) \in U$ and for every $Ra_f^0 < Ra_f < Ra_f^0 + \epsilon$ with some $\epsilon > 0$, the solution to the equations (2.5)–(2.7), given by*

$$\psi = (\mathbf{v}_f(x,z,t), \theta_f(x,z,t), \mathbf{v}_m(x,z,t), \theta_m(x,z,t))$$

satisfies

$$\limsup_{t\to+\infty} ||\psi||_{\mathbf{Y}} \geq \delta > 0.$$

for some δ independent of Ra_f.

Remark 4.1. *In the case $P = 0$ or very small, one needs to calculate higher-order approximations of the center manifold function. A transition theorem can be established in principle.*

5 Numerical evaluation of the transition number and discussion

In this section we numerically compute the transition number P whose sign determines the transition (bifurcation) type according to Theorem 4.1 pertaining to the dynamic transition of thermal convection in superposed fluid and porous layers as the Rayleigh number in porous media Ra_m varies. These numerical results have been validated through tests of grid refinement.

In Fig. 4, we plot the transition number as a function of the height ratio (left panel) and aspect ratio (right panel), respectively. One observes that the transition number P remains negative for most values of $\hat{d}$ and b. According to Theorem 4.1 this suggests that the perturbed system (2.9)-(2.11) prefers a continuous transition (attractor bifurcation) at the critical Rayleigh number. Note for $b = 1.5$ there are certain positive P when the height ratio $\hat{d}$ is close to 0.13, indicating that a jump transition occurs at those particular height ratio. We point out that jump transitions of $P > 0$ are not observed in the classical Rayleigh-Bé problem in a single domain, cf. [22, 32, 40, 41]. The interplay between convection in free flow and convection in porous media can indeed incur jump transitions in certain parameter regimes. One also observes that the transition number jumps when it crosses the value zero. As we noted in Remark 4.1 at $P = 0$ one needs to compute the coefficients of the fourth order terms in the reduced equation (4.46) in order to determine the type of transitions.

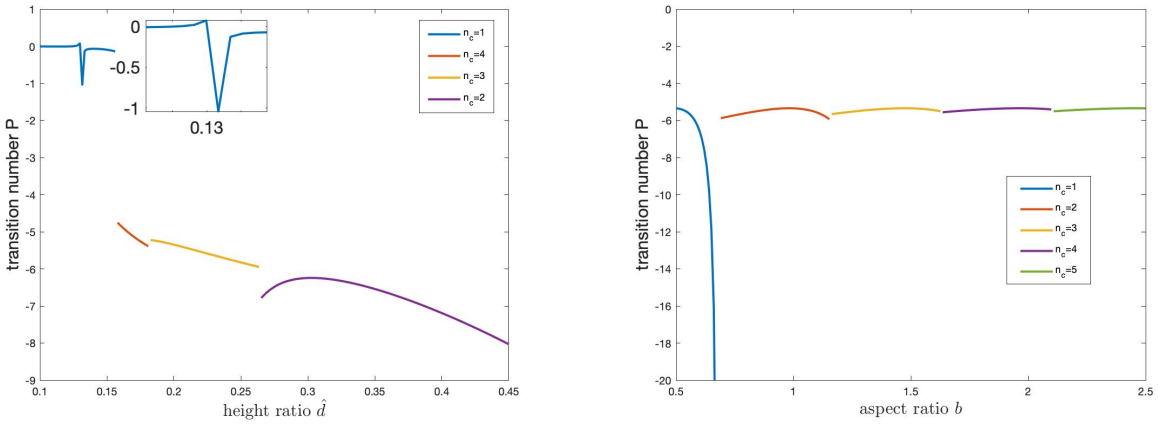

Figure 4: Plot of transition number as a function of height ratio (left) and aspect ratio (right), respectively. The parameters are: $Pr_f = 6$; $\alpha = 1$; $\rho = 10$, $\epsilon_T = 0.7$, $\chi = 0.3$, $Da = 25 \times 10^{-6}$, $b = 1.5$, $\hat{d} = 0.2$.

We further observe from Fig. 4 that the transition number has jump discontinuities at those values of $\hat{d}$ and b-hereafter denoted by $\hat{d}_j$ and b_j-where the critical mode n_c changes value. Recall from the discussion in subsection 3.2 that at these $\hat{d}_j$ and b_j two or more eigenvalues of the eigenvalue problem (3.34) simultaneously cross the imaginary axis. Hence the transition type can not be determined by the transition number P because the reduced equation (4.68) is not applicable at these discontinuities. By Theorem 4.1 a bifurcated solution has the approximate expression

$$(\mathbf{v}_f, \theta_f, \mathbf{v}_m, \theta_m) \approx x\,\mathrm{Re}(\psi^p) + y\,\mathrm{Im}(\psi^p), \quad x^2 + y^2 = -\frac{\sigma_1}{P},$$

away from the $\hat{d}_j$s and b_js. Owing to the jump discontinuities of P at these points, one infers that the bifurcated solutions undergo a jump transition at these $\hat{d}_j$s and b_js if one views $\hat{d}$ and b as the control parameters, respectively. Since n_c changes values at these location, the number of rolls changes in the physical space. This phenomena of jump transition is illustrated in Fig. 5 where the flow changes from two rolls for $\hat{d} = 0.15$ to eight rolls for $\hat{d} = 0.18$, which is consistent with the change of n_c in the left panel shown in Fig. 4.

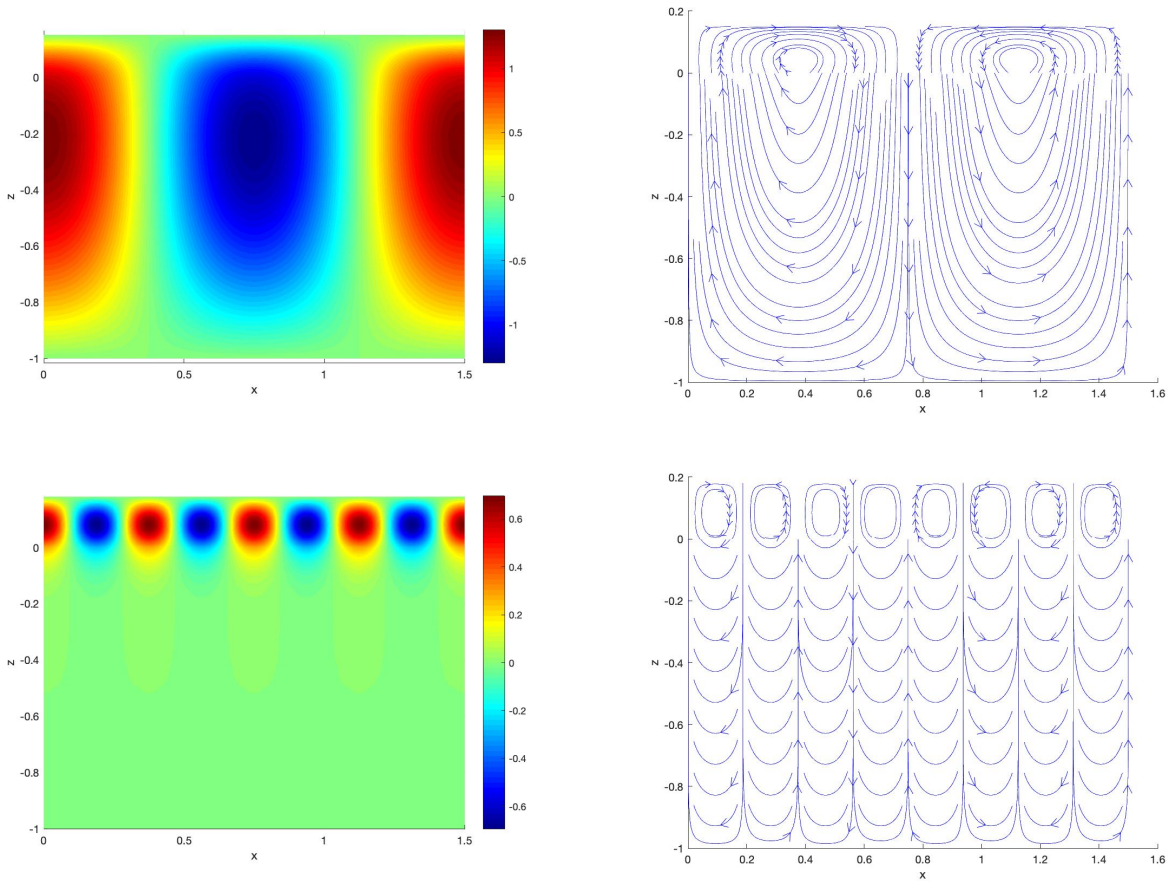

Figure 5: The approximate bifurcated solutions–temperature (left), streamline of flow field (right)–at height ratio $\hat{d} = 0.15$ (first row) and $\hat{d} = 0.18$ (second row), respectively. The parameters are: $Pr_f = 6$; $\alpha = 1$; $\rho = 10$, $\epsilon_T = 0.7$, $\chi = 0.3$, $Da = 25 \times 10^{-6}$, $b = 1.5$.

Note that for fixed d_m and b as in Fig. 5, n_c (proportional to the wave number) provides the length scale of the convection rolls, that is the larger n_c corresponds to smaller convection rolls. In contrast to $\hat{d}_j, j = 2, 3$, the critical mode n_c jumps from 1 to 4 across $\hat{d}_1$, which signals a dramatic flow regime change from full convection where the convection rolls extend throughout the entire domain to free-flow dominated convection in which the convection cells are mainly confined in the free flow region. This phenomena is first observed numerically in [36] for $b = 3$. Fig. 6 demonstrates this case where one observes the flow regime changes from full convection (2 rolls) to free-flow dominated convection (14 rolls). Note that the transitions are all of continuous type except at the jump discontinuities $\hat{d}_j$.

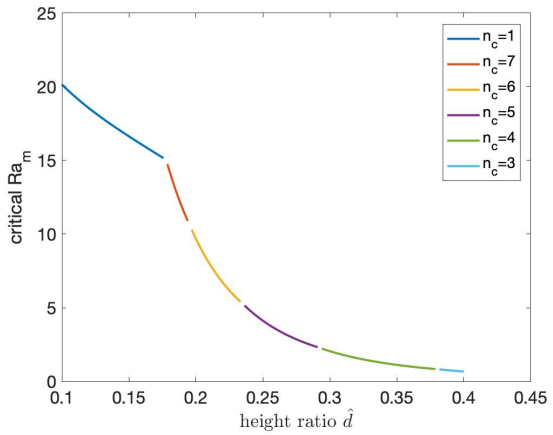

neutral stability curve

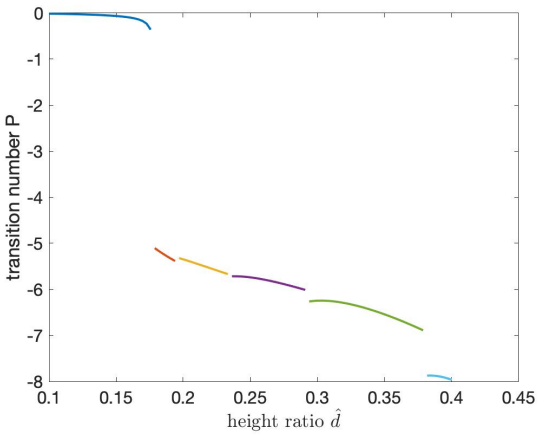

transition number plot

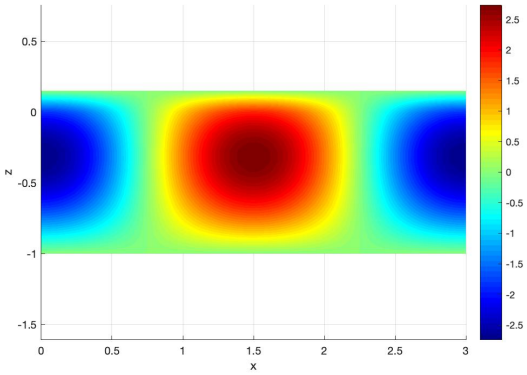

temperature $\hat{d} = 0.15$

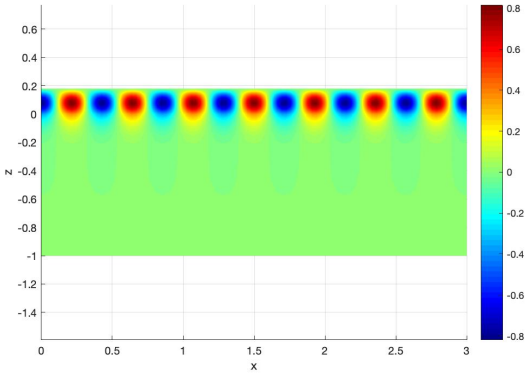

temperature $\hat{d} = 0.18$

Figure 6: Transition from full convection to free-flow dominated convection. The parameters are: $Pr_f = 6$; $\alpha = 1$; $\rho = 10$, $\epsilon_T = 0.7$, $\chi = 0.3$, $Da = 25 \times 10^{-6}$, $b = 3$.

We also investigate the effect of the Darcy number Da and the thermal diffusivity ϵ_T on the onset of thermal convection and the structure of the convection cells. Fig. 7 shows the plots of neutral stability curve and the transition number, respectively, as a function of Da. One observes that both the critical Rayleigh number and the transition number monotonically increase as the Darcy number does, until it levels off. Recall that the Darcy model employed here is suitable for the regime of small Darcy number. In terms of transition, one notices a sharp jump transition at Da_2 (second jump discontinuity) where the flow configuration changes from free-flow dominated convection to full convection. Furthermore, the transitions after Da_2 are of jump type ($P > 0$). Similar effects are also observed for the thermal diffusivity ratio ϵ_T in Fig. 8, though transitions are continuous except at the jump discontinuities.

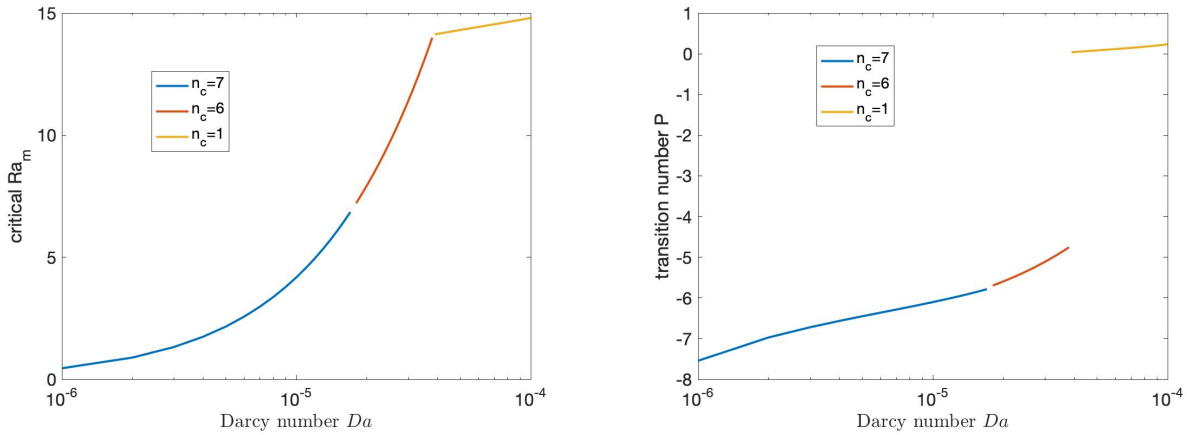

Figure 7: Neutral stability curve (left) and plot of transition number as a function of Darcy number (right). The parameters are: $Pr_f = 6$; $\alpha = 1$; $\rho = 10$, $\epsilon_T = 0.7$, $\chi = 0.3$, , $b = 3$, $\hat{d} = 0.2$.

6 Conclusion

In this article we perform a thorough analysis in terms of bifurcation and dynamic transitions for thermal convection in a fluid layer overlying a saturated porous medium based on a two-dimensional Navier-Stokes-Darcy-Boussinesq model. A transition theorem with an explicit transition number is deduced by reducing the infinite dynamical system onto the center manifold. We show by careful numerical evaluation of the transition number that the system is in favour of a continuous transition in which the steady state solution bifurcates to a local attractor at the critical Rayleigh number. Jump transitions can occur at certain parameter regime. In particular the jump transition corresponds to the change of flow regime from full convection to free-flow dominated convection at discontinuities of the transition number as a function of the ratio of free-flow to porous media depth, the Darcy number or the thermal diffusivity ratio.

The results in this article can be extended in several directions which we will pursue in future works. Note that the time derivative of the Darcy velocity is present in our model. Since the Darcy number is small in the regime that we are interested in, we would like to consider the classical Darcy equation neglecting this term. Secondly, we would like to establish the PES condition for generic ϵ_T. Finally it would be interesting to consider the convection problem in three-dimension and with other physical boundary conditions.

Acknowledgement

D. Han acknowledges support from the National Science Foundation grant DMS-1912715. The work of Q. Wang. is supported by the National Science Foundation of China (NSFC) grant No. 11901408. X. Wang acknowledges support from

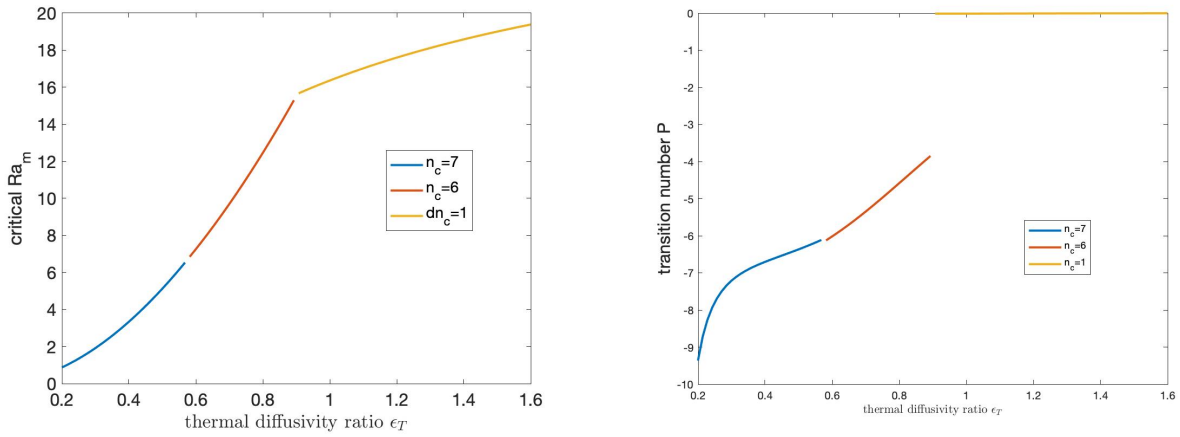

Figure 8: Neutral stability curve (left) and plot of transition number as a function of thermal diffusivity ratio (right). The parameters are: $Pr_f = 6$; $\alpha = 1$; $\rho = 10$, $Da = 25 \times 10^{-6}$, $\chi = 0.3$, , $b = 3$, $\hat{d} = 0.2$.

References

[1] Myron B. Allen. *Collocation Techniques for Modeling Compositional Flows in Oil Reservoirs*. Springer, New York, 1984.

[2] J. Bear. *Dynamics of fluids in porous media*. Courier Dover Publications, Sep 1,1988.

[3] Gordon S. Beavers and Daniel D. Joseph. Boundary conditions at a naturally permeable wall. *Journal of Fluid Mechanics*, 30(1):197207, 1967.

[4] F. Boano, J. W. Harvey, A. Marion, A. I. Packman, R. Revelli, L. Ridolfi, and A. Wrman. Hyporheic flow and transport processes: Mechanisms, models, and biogeochemical implications. *Reviews of Geophysics*, 52(4):603–679, 2014.

[5] Myron B. Allen Brian J. Suchomel, Benito M. Chen. Network model of flow, transport and biofilm effects in porous media. *Numer. Methods Partial Differential Equations*, 30(1):1–23, 1998.

[6] M. Bayani Cardenas. Hyporheic zone hydrologic science: A historical account of its emergence and a prospectus. *Water Resources Research*, 51(5):3601–3616, 2015.

[7] Magda Carr. Penetrative convection in a superposed porous-medium-fluid layer via internal heating. *J. Fluid Mech.*, 509:305–329, 2004.

[8] Min-Hsing Chang. Thermal convection in superposed fluid and porous layers subjected to a horizontal plane couette flow. *Physics of Fluids*, 17(6):064106, 2005.

[9] Min-Hsing Chang. Thermal convection in superposed fluid and porous layers subjected to a plane Poiseuille flow. *Phys. Fluids*, 18(3):035104, 10, 2006.

[10] Mickaël D. Chekroun and Honghu Liu. Finite-horizon parameterizing manifolds, and applications to suboptimal control of nonlinear parabolic PDEs. *Acta Appl. Math.*, 135:81–144, 2015.

[11] Mickaël D. Chekroun, Honghu Liu, and Shouhong Wang. *Approximation of stochastic invariant manifolds.* SpringerBriefs in Mathematics. Springer, Cham, 2015. Stochastic manifolds for nonlinear SPDEs. I.

[12] Mickaël D. Chekroun, Honghu Liu, and Shouhong Wang. *Stochastic parameterizing manifolds and non-Markovian reduced equations.* SpringerBriefs in Mathematics. Springer, Cham, 2015. Stochastic manifolds for nonlinear SPDEs. II.

[13] B. Chen, A. Cunningham, R. Ewing, R. Peralta, and E. Visser. Two-dimensional modeling of microscale transport and biotransformation in porous media. *Numer. Methods Partial Differential Equations*, 10(1):65–83, 1994.

[14] Falin Chen and C. F. Chen. Convection in superposed fluid and porous layers. *Journal of Fluid Mechanics*, 234:97119, 1992.

[15] Vladimir V. Chepyzhov and Mark I. Vishik. *Attractors for equations of mathematical physics*, volume 49 of *American Mathematical Society Colloquium Publications.* American Mathematical Society, Providence, RI, 2002.

[16] Henk Dijkstra, Taylan Sengul, Jie Shen, and Shouhong Wang. Dynamic transitions of quasi-geostrophic channel flow. *SIAM J. Appl. Math.*, 75(5):2361–2378, 2015.

[17] Marco Discacciati and Alfio Quarteroni. Navier-Stokes/Darcy coupling: modeling, analysis, and numerical approximation. *Rev. Mat. Complut.*, 22(2):315–426, 2009.

[18] P. G. Drazin. *Introduction to hydrodynamic stability.* Cambridge Texts in Applied Mathematics. Cambridge University Press, Cambridge, 2002.

[19] Richard E. Ewing and Suzanne L. Weekes. Numerical methods for contaminant transport in porous media. In *Advances in computational mathematics (Guangzhou, 1997)*, volume 202 of *Lecture Notes in Pure and Appl. Math.*, pages 75–95. Dekker, New York, 1999.

[20] Quarteroni A. Veneziani A. Formaggia, L. *Cardiovascular mathematics: modeling and simulation of the circulatory system.* Springer-Verlag, New York, 2009.

[21] Călin-Ioan Gheorghiu. *Spectral methods for non-standard eigenvalue problems.* SpringerBriefs in Mathematics. Springer, Cham, 2014. Fluid and structural mechanics and beyond.

[22] Daozhi Han, Marco Hernandez, and Quan Wang. Dynamic bifurcation and transition in the Rayleigh-Bénard convection with internal heating and varying gravity. *Commun. Math. Sci.*, 17(1):175–192, 2019.

[23] A.A. Hill and B. Straughan. Poiseuille flow in a fluid overlying a highly porous material. *Advances in Water Resources*, 32(11):1609 – 1614, 2009.

[24] Antony A. Hill and Magda Carr. Nonlinear stability of the one-domain approach to modelling convection in superposed fluid and porous layers. *Proc. R. Soc. Lond. Ser. A Math. Phys. Eng. Sci.*, 466(2121):2695–2705, 2010.

[25] Antony A. Hill and Brian Straughan. Global stability for thermal convection in a fluid overlying a highly porous material. *Proc. R. Soc. Lond. Ser. A Math. Phys. Eng. Sci.*, 465(2101):207–217, 2009.

[26] S.C. Hirata, B. Goyeau, D. Gobin, M. Chandesris, and D. Jamet. Stability of natural convection in superposed fluid and porous layers: Equivalence of the one- and two-domain approaches. *International Journal of Heat and Mass Transfer*, 52(1):533 – 536, 2009.

[27] Chun-Hsiung Hsia, Chang-Shou Lin, Tian Ma, and Shouhong Wang. Tropical atmospheric circulations with humidity effects. *Proc. A.*, 471(2173):20140353, 24, 2015.

[28] I. P. Jones. Low reynolds number flow past a porous spherical shell. *Mathematical Proceedings of the Cambridge Philosophical Society*, 73(1):231238, 1973.

[29] Honghu Liu, Taylan Sengul, and Shouhong Wang. Dynamic transitions for quasilinear systems and Cahn-Hilliard equation with Onsager mobility. *J. Math. Phys.*, 53(2):023518, 31, 2012.

[30] Honghu Liu, Taylan Sengul, Shouhong Wang, and Pingwen Zhang. Dynamic transitions and pattern formations for a Cahn-Hilliard model with long-range repulsive interactions. *Commun. Math. Sci.*, 13(5):1289–1315, 2015.

[31] T. P. Lyubimova and E. A. Kolchanova. The onset of double-diffusive convection in a superposed fluid and porous layer under high-frequency and small-amplitude vibrations. *Transp. Porous Media*, 122(1):97–124, 2018.

[32] Tian Ma and Shouhong Wang. Rayleigh-Bénard convection: dynamics and structure in the physical space. *Commun. Math. Sci.*, 5(3):553–574, 2007.

[33] Tian Ma and Shouhong Wang. Principle of exchange of stabilities and dynamic transitions. *Georgian Math. J.*, 15(3):581–590, 2008.

[34] Tian Ma and Shouhong Wang. Cahn-Hilliard equations and phase transition dynamics for binary systems. *Discrete Contin. Dyn. Syst. Ser. B*, 11(3):741–784, 2009.

[35] Tian Ma and Shouhong Wang. *Phase transition dynamics*. Springer, New York, 2014.

[36] Matthew McCurdy, Nicholas Moore, and Xiaoming Wang. Convection in a coupled free flow-porous media system. *SIAM J. Appl. Math.*, 79(6):2313–2339, 2019.

[37] Donald A. Nield and Adrian Bejan. *Convection in porous media*. Springer-Verlag, New York, second edition, 1999.

[38] P. G. Saffman. On the boundary condition at the surface of a porous medium. *Studies in Applied Mathematics*, 50(2):93–101, 1971.

[39] George R. Sell and Yuncheng You. *Dynamics of evolutionary equations*, volume 143 of *Applied Mathematical Sciences*. Springer-Verlag, New York, 2002.

[40] Taylan Sengul, Jie Shen, and Shouhong Wang. Pattern formations of 2D Rayleigh-Bénard convection with no-slip boundary conditions for the velocity at the critical length scales. *Math. Methods Appl. Sci.*, 38(17):3792–3806, 2015.

[41] Taylan Sengul and Shouhong Wang. Pattern formation in Rayleigh-Bénard convection. *Commun. Math. Sci.*, 11(1):315–343, 2013.

[42] B. Straughan. Effect of property variation and modelling on convection in a fluid overlying a porous layer. *International Journal for Numerical and Analytical Methods in Geomechanics*, 26(1):75–97, 2001.

[43] S. P. Suma, Y. H. Gangadharaiah, R. Indira, and I. S. Shivakumara. Throughflow effects on penetrative convection in superposed fluid and porous layers. *Transp. Porous Media*, 95(1):91–110, 2012.

[44] Roger Temam. *Infinite-dimensional dynamical systems in mechanics and physics*, volume 68 of *Applied Mathematical Sciences*. Springer-Verlag, New York, second edition, 1997.

[45] Mary F. Wheeler, editor. *Numerical simulation in oil recovery*, volume 11 of *The IMA Volumes in Mathematics and its Applications*. Springer-Verlag, New York, 1988. Papers from the workshop held at the University of Minnesota, Minneapolis, Minn., December 1–12, 1986.